

Reactions of the Dinuclear Ruthenium Complex $\{(\eta^5\text{-C}_5\text{H}_3)_2(\text{SiMe}_2)_2\}\text{Ru}_2(\text{CO})_4$, Featuring a Doubly Linked Dicyclopentadienyl Ligand

Maxim V. Ovchinnikov,[†] David P. Klein,[†] Ilia A. Guzei,[‡] Moon-Gun Choi,[§] and Robert J. Angelici^{*,†}

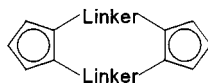
Department of Chemistry and Molecular Structure Laboratory, Iowa State University, Ames, Iowa 50011, and Department of Chemistry and Molecular Structure Laboratory, Yonsei University, Seoul, Korea 120-749

Received July 27, 2001

The complex $\{(\eta^5\text{-C}_5\text{H}_3)_2(\text{SiMe}_2)_2\}\text{Ru}_2(\text{CO})_4$ (**1**), which features the doubly linked dicyclopentadienyl ligand $(\eta^5\text{-C}_5\text{H}_3)_2(\text{SiMe}_2)_2$, reacts with phosphines (PMe_3 , PCy_3 , PPh_3) to give $\{(\eta^5\text{-C}_5\text{H}_3)_2(\text{SiMe}_2)_2\}\text{Ru}_2(\text{CO})(\mu\text{-CO})_2(\text{PR}_3)$ (**2a–c**), with halogens X_2 ($\text{X} = \text{Cl}, \text{Br}, \text{I}$) to give the Ru–Ru-cleaved products $\{(\eta^5\text{-C}_5\text{H}_3)_2(\text{SiMe}_2)_2\}\text{Ru}_2(\text{CO})_4(\text{X})_2$ (**3a–c**), with X_2 and AgTfO to give $[\{(\eta^5\text{-C}_5\text{H}_3)_2(\text{SiMe}_2)_2\}\text{Ru}_2(\text{CO})_4(\mu\text{-X})]^+\text{TfO}^-$ ($\text{X} = \text{Cl}, \text{Br}, \text{I}$; **4a–c**), and with SnCl_2 to give $\{(\eta^5\text{-C}_5\text{H}_3)_2(\text{SiMe}_2)_2\}\text{Ru}_2(\text{CO})_4(\mu\text{-SnCl}_2)$ (**5**), resulting from the insertion of SnCl_2 into the Ru–Ru bond. Reduction of **1** with Na/Hg generates $[\{(\eta^5\text{-C}_5\text{H}_3)_2(\text{SiMe}_2)_2\}\text{Ru}_2(\text{CO})_4]^{2-}$ (**6**), which reacts with $(\eta^5\text{-C}_5\text{H}_5)_2\text{TiCl}_2$ to give $\{(\eta^5\text{-C}_5\text{H}_3)_2(\text{SiMe}_2)_2\}\text{Ru}_2(\text{CO})_4\{\mu\text{-Ti}(\eta^5\text{-C}_5\text{H}_5)_2\}$ (**7**). Ultraviolet photolysis of **1** with diphenylacetylene and phenylacetylene yields a series of five dinuclear Ru complexes (**8–10**, **12**, **13**) containing one or two bridging acetylene units. The rigidity of the doubly linked $(\eta^5\text{-C}_5\text{H}_3)_2(\text{SiMe}_2)_2$ ligand substantially influences the reactivity and structures of the complexes. Molecular structures of **1**, **2a**, **3c**, **5**, **9**, **10**, and **12** as determined by X-ray diffraction studies are also presented.

Introduction

The doubly linked bis(cyclopentadienyl) ligands $(\eta^5\text{-C}_5\text{H}_3)(\text{Linker})_2$ ($\text{Linker} = \text{CH}, \text{CH}_2, \text{CH}_2\text{CH}_2, \text{SiMe}_2, \text{GeMe}_2$, etc.) have been extensively explored as frameworks for dinuclear metal complexes that are resistant to fragmentation and have two metal centers in close proximity.¹



The latter feature is especially attractive for studying cooperative effects between two reactive metal sites, since free rotation cannot occur around the Cp–(Linker)₂–Cp linker unit. Most of the known $(\eta^5\text{-C}_5\text{H}_3)_2\text{-}(\text{SiMe}_2)_2$ -bridged bimetallic complexes contain group 4²

or 6³ metals. To the best of our knowledge, only one example of a nonmetallocene complex $(\{(\eta^5\text{-C}_5\text{H}_3)_2(\text{SiMe}_2)_2\}\text{Fe}_2(\text{CO})_4)$ is known for group 8 metals,^{4a} and little chemistry of this compound has been reported.

We recently reported⁵ the synthesis (Scheme 1) of the cationic dinuclear complex $[\{(\eta^5\text{-C}_5\text{H}_3)_2(\text{SiMe}_2)_2\}\text{Ru}_2(\text{CO})_4(\mu\text{-H})]^+$ (**1H**⁺), whose carbon monoxide ligands are activated to attack by amine nucleophiles because of the positive charge on the complex and the slow rate of deprotonation of the bridging hydride by the amines.

To develop a general understanding of the effect of the doubly linked $(\eta^5\text{-C}_5\text{H}_3)_2(\text{SiMe}_2)_2$ ligand on the reactivity of $\{(\eta^5\text{-C}_5\text{H}_3)_2(\text{SiMe}_2)_2\}\text{Ru}_2(\text{CO})_4$ (**1**), we have explored the reactions of **1** with phosphines, halogens, SnCl_2 , Na/Hg, phenylacetylene, and diphenylacetylene to give a variety of new complexes. These reactions also demonstrate the robustness of the bridging system, which remains unchanged throughout the transformations.

* To whom correspondence should be addressed. E-mail: angelici@iastate.edu.

[†] Department of Chemistry, Iowa State University.

[‡] Molecular Structure Laboratory, Iowa State University.

[§] Yonsei University, Molecular Structure Laboratory.

(1) For general reviews of linked bis(cyclopentadienyl) organometallic complexes, see: (a) Barlow, S.; O'Hare, D. *Chem. Rev.* **1997**, *97*, 637. (b) Werner, H. *Inorg. Chim. Acta* **1992**, *198–200*, 715. (c) Bonifaci, C.; Cecon, A.; Gambaro, A.; Mantovani, L.; Ganis, P.; Santi, S.; Venzo, A. *J. Organomet. Chem.* **1998**, *557*, 97. (d) Cuenca, T.; Royo, P. *Coord. Chem. Rev.* **1999**, *193–195*, 447. (e) Royo, P. *New J. Chem.* **1997**, *21*, 791.

(2) (a) Gómez-García, R.; Royo, P. *J. Organomet. Chem.* **1999**, *583*, 86. (b) Cano, A.; Cuenca, T.; Gómez-Sal, P.; Royo, B.; Royo, P. *Organometallics* **1994**, *13*, 1688. (c) Corey, J. Y.; Huhmann, J. L.; Rath, N. P. *Inorg. Chem.* **1995**, *34*, 3203. (d) Cano, A. M.; Cano, J.; Cuenca, T.; Gómez-Sal, P.; Manzanero, A.; Royo, P. *Inorg. Chim. Acta* **1998**, *280*, 1.

(3) (a) Amor, F.; Gómez-Sal, P.; de Jesús, E.; Royo, P.; Vázquez de Miguel, A. *Organometallics* **1994**, *13*, 4322. (b) Amor, F.; de Jesús, E.; Pérez, A. I.; Royo, P.; Vázquez de Miguel, A. *Organometallics* **1996**, *15*, 365. (c) Amor, F.; de Jesús, E.; Royo, P.; Vázquez de Miguel, A. *Inorg. Chem.* **1996**, *35*, 3440. (d) Galakhov, M. V.; Gil, A.; de Jesús, E.; Royo, P. *Organometallics* **1995**, *14*, 3746. (e) Amor, F.; Gómez-Sal, P.; de Jesús, E.; Martín, A.; Pérez, A. I.; Royo, P.; Vázquez de Miguel, A. *Organometallics* **1996**, *15*, 2103. (f) Calvo, M.; Galakhov, M. V.; Gómez-García, R.; Gómez-Sal, P.; Martín, A.; Royo, P.; Vázquez de Miguel, A. *J. Organomet. Chem.* **1997**, *548*, 157.

(4) (a) Siemeling, U.; Jutzi, P.; Neumann, B.; Stammer, H. G.; Hursthouse, M. B. *Organometallics* **1992**, *11*, 1328. (b) Hiermeier, J.; Koehler, F. H.; Mueller, G. *Organometallics* **1991**, *10*, 1787.

(5) (a) Ovchinnikov, M. V.; Angelici, R. J. *J. Am. Chem. Soc.* **2000**, *122*, 6130. (b) Ovchinnikov, M. V.; Guzei, I. A.; Angelici, R. J. *Organometallics* **2001**, *20*, 691.

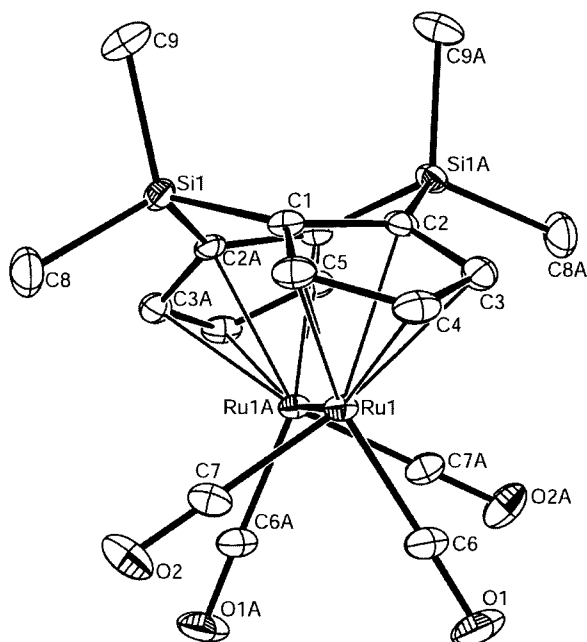
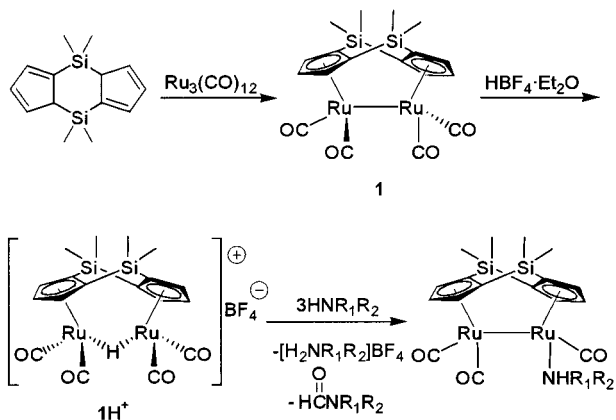


Figure 1. Thermal ellipsoid drawing of $\{(\eta^5\text{-C}_5\text{H}_3)_2(\text{SiMe}_2)_2\}\text{Ru}_2(\text{CO})_4$ (**1**) showing the labeling scheme and 30% probability ellipsoids. Hydrogens are omitted for clarity. Selected bond distances (Å) and angles (deg) are as follows: Ru(1)–Ru(1A), 2.8180(3); Ru(1)–C(6), 1.868(2); Ru(1)–C(7), 1.854(2); Ru(1)–Cp(centroid), 1.907; $\angle\text{C}(6)\text{–Ru}(1)\text{–C}(7)$, 87.45(9); $\angle\text{Ru}(1\text{A})\text{–Ru}(1)\text{–C}(6)$, 93.04(7); $\angle\text{Ru}(1\text{A})\text{–Ru}(1)\text{–C}(7)$, 85.15(6); $\angle\text{Cp(centroid)}\text{–Ru}(1)\text{–Ru}(1\text{A})\text{–Cp(centroid)}$, 24.2; $\angle\text{C}(7)\text{–Ru}(1)\text{–Ru}(1\text{A})\text{–C}(6\text{A})$, 32.3; $\angle\text{Cp–Cp fold angle}$, 122.86.

Scheme 1



Results and Discussion

Crystal Structure of $\{(\eta^5\text{-C}_5\text{H}_3)_2(\text{SiMe}_2)_2\}\text{Ru}_2(\text{CO})_4$ (1**).** The starting complex **1**, whose synthesis (Scheme 1) was recently reported,⁵ has a structure (Figure 1, Table 1) that contains two ruthenium atoms linked by a bridging $(\eta^5\text{-C}_5\text{H}_3)_2(\text{SiMe}_2)_2$ ligand and a metal–metal bond, with four terminal CO ligands bound in a symmetrical and staggered array ($\angle\text{C}(7)\text{–Ru}(1)\text{–Ru}(1\text{A})\text{–C}(6\text{A}) = 32.3^\circ$). The staggered character of the molecule is also reflected by a significant twist around the Ru(1)–Ru(1A) axis ($\angle\text{Cp(centroid)}\text{–Ru}(1)\text{–Ru}(1\text{A})\text{–Cp(centroid)} = 24.2^\circ$). The fold angle between the planes of the Cp rings of the $(\eta^5\text{-C}_5\text{H}_3)_2(\text{SiMe}_2)_2$ ligand is relatively large (122.86°), suggesting that the normally planar $(\eta^5\text{-C}_5\text{H}_3)_2(\text{SiMe}_2)_2$ fragment (e.g. in *trans*- $\{(\eta^5\text{-C}_5\text{H}_3)_2(\text{SiMe}_2)_2\}\text{Li}_2(\text{TMEDA})_2$)^{4b} is somewhat strained, leading

to a longer than normal Ru–Ru single bond distance. The Ru–Ru distance (2.821(1) Å) in $(\eta^5\text{-}\eta^5\text{-fulvalene})\text{-Ru}_2(\text{CO})_4$,⁶ where fulvalene is $\eta^5\text{-}\eta^5\text{-C}_5\text{H}_4\text{-C}_5\text{H}_4$, is also significantly greater than that in the corresponding nonlinked complex $\text{Cp}_2\text{Ru}_2(\mu\text{-CO})_2(\text{CO})_2$ (2.735(2) Å).⁷ Avoidance of nonbonding interactions between the carbonyl ligands and alleviation of strain by decreasing the $\eta^5\text{-}\eta^5\text{-fulvalene}$ bend were cited to account for this lengthened Ru–Ru bond. In part, similar arguments may be applied to **1**. Thus, the Ru–Ru distance in **1** (2.8180(3) Å) is longer than that observed in $\text{Cp}_2\text{Ru}_2(\text{CO})_2(\mu\text{-CO})_2$ (2.735(2) Å). This difference is partially due to the preference of the carbonyl ligands in **1** for an all-terminal arrangement that favors a longer Ru–Ru distance, which also relieves the strain in the folded $(\eta^5\text{-C}_5\text{H}_3)_2(\text{SiMe}_2)_2$ ligand. Avoidance of nonbonding contacts between the carbonyl ligands is probably also responsible for elongation of the Ru–Ru bond and for the staggered conformation of the CO ligands in **1**. It is worth noting that $(\eta^5\text{-}\eta^5\text{-fulvalene})\text{Ru}_2(\text{CO})_4$ adopts an eclipsed conformation of the CO ligands, presumably because the twist around the Ru–Ru axis would lead to an energetically unfavorable further elongation of the Ru–Ru bond and/or to an increase in the nonplanarity of the $\eta^5\text{-}\eta^5\text{-fulvalene}$ ligand.

Substitution of a CO in **1 by Phosphines.** Complex **1** reacts at 200 °C with phosphines PR_3 (R = Me, Cy, Ph) to give monosubstituted complexes of the type $\{(\eta^5\text{-C}_5\text{H}_3)_2(\text{SiMe}_2)_2\}\text{Ru}_2(\text{CO})(\mu\text{-CO})_2(\text{PR}_3)$ (**2**), where R = Me (**2a**), R = Cy (**2b**), R = Ph (**2c**) (Scheme 2). No disubstituted products were observed. Also, it is worth noting that the same reaction did not give the clean formation of **2a** under UV photolysis conditions. The IR spectra of **2a–c** in CH_2Cl_2 exhibit $\nu(\text{CO})$ bands at 1977–1967, 1946–1935, 1917–1907, and 1745–1733 cm^{-1} , consistent with the presence of both terminal and bridging isomers of **2a–c** in solution. Absorbances in the ranges 1977–1967 and 1917–1907 cm^{-1} indicate the presence of the terminal isomer, while absorbances between 1946–1935 and 1745–1733 cm^{-1} correspond to the bridging isomer. More of the terminal isomer of **2a–c** is observed in the low-polarity solvent hexanes than in CH_2Cl_2 . The IR spectrum of **2a** in the solid state shows approximately equal amounts of the bridging and nonbridging isomers. The crystal used for the molecular structure determination of **2a** was picked from a mixture of both isomers. The molecular structure of **2a** determined by X-ray diffraction (Figure 2, Table 1) shows an almost symmetrical disposition of the bridging CO ligands, which are responsible for the shorter Ru(1)–Ru(2) distance (2.6579(2) Å) compared to that observed in **1** (2.8180(3) Å) and, surprisingly, to that observed in $\text{Cp}_2\text{Ru}_2(\text{CO})(\mu\text{-CO})_2(\text{PMe}_3)$ (2.722(2) Å).⁸ The shorter Ru(1)–Ru(2) distance in **2a** may also be favored by the doubly linked $(\eta^5\text{-C}_5\text{H}_3)_2(\text{SiMe}_2)_2$ ligand, which adopts a smaller $\angle\text{Cp–Cp fold angle}$ (119.0°), compared to that (122.86°) in complex **1**, which relieves unfavorable steric interactions between the bridging CO ligands and the equatorial SiMe₂ methyl groups. This argument is also supported by the smaller dihedral angle between

(6) Boese, R.; Cammack, J. K.; Matzger, A. J.; Pflug, K.; Tolman, W. B.; Vollhardt, K. P. C.; Weidman, T. W. *J. Am. Chem. Soc.* **1997**, *119*, 6757.

(7) Mills, D. S.; Nice, J. P. *J. Organomet. Chem.* **1967**, *9*, 339.

(8) Nataro, C.; Angelici, R. J. *Inorg. Chem.* **1998**, *37*, 2975.

Table 1. Crystallographic Data for 1, 2a, 3c, 5, 9, 10, and 12

	1	2a	3c	5	9	10	12
formula	C ₁₈ H ₁₈ O ₄ Ru ₂ Si ₂	C ₂₀ H ₂₇ O ₃ PRu ₂ Si ₂ ·1/2C ₆ H ₁₄	C ₁₈ H ₁₈ I ₂ O ₄ Ru ₂ Si ₂	C ₁₈ H ₁₈ Cl ₂ O ₄ Ru ₂ Si ₂ Sn	C ₄₃ H ₃₈ ORu ₂ Si ₂	C ₄₄ H ₃₈ O ₂ Ru ₂ Si ₂ ·1/2CH ₂ Cl ₂	C ₂₅ H ₂₄ O ₃ Ru ₂ Si ₂ ·CH ₂ Cl ₂
fw	556.64	647.79	810.44	746.23	829.05	899.53	715.69
cryst syst	monoclinic	monoclinic	monoclinic	monoclinic	trigonal	trigonal	monoclinic
space group	C2/c	P2 ₁ /c	P2 ₁	P2 ₁ /c	P1	P1	P2 ₁ /c
a, Å	15.1911(9)	10.3672(4)	9.0042(4)	17.5165(10)	12.5711(16)	8.6733(14)	18.8600(8)
b, Å	10.1057(6)	17.6827(7)	39.9004(16)	17.0163(10)	12.7517(16)	12.709(2)	9.6259(5)
c, Å	14.3573(9)	15.2779(6)	10.1932(4)	24.5775(14)	12.7791(16)	35.391(6)	15.3656(11)
α, deg	90	90	90	90	99.449(2)	96.629(3)	90
β, deg	113.475(1)	109.273(1)	91.4325(10)	93.123(1)	111.366(2)	96.898(3)	92.119(1)
γ, deg	90	90	90	90	92.545(2)	93.476(3)	90
V, Å ³	2021.7(2)	2643.78(18)	3661.0(3)	7314.8(7)	1869.7(4)	3835.9(11)	2787.6(3)
Z	4	4	6	12	2	4	4
cryst color, habit	yellow block	yellow block	yellow block	yellow block	orange plate	dark red rod	orange plate
cryst size, mm	0.38 × 0.34 × 0.32	0.40 × 0.30 × 0.30	0.40 × 0.35 × 0.30	0.45 × 0.40 × 0.40	0.36 × 0.12 × 0.04	0.55 × 0.12 × 0.06	0.43 × 0.35 × 0.03
D(calcd), g cm ⁻³	1.829	1.627	2.206	2.033	1.473	1.558	1.705
wavelength, Å							
μ(Mo Kα), mm ⁻¹	1.632	1.315	3.886	2.578	0.904	0.957	1.387
temp, K	293(2)	173(2)	173(2)	273(2)	233(2)	293(2)	173(2)
diffractometer							
abs cor							
θ range, deg	2.49–26.37	1.82–26.37	1.02–26.37	1.16–28.28	1.74–23.00	1.62–25.15	2.38–25.00
no. of rflns collected	8075	22 306	30 328	64 369	11 583	28 494	9719
no. of indep rflns (R(int))	2063 (0.0181)	5374 (0.0208)	14717 (0.0309)	17373 (0.0448)	5186 (0.0487)	13641 (0.0525)	4849 (0.0450)
R(F) (I ≥ 2σ(I)), %	R1 = 0.0174, wR2 = 0.0457	R1 = 0.0204, wR2 = 0.0532	R1 = 0.0293, wR2 = 0.0570	R1 = 0.0301, wR2 = 0.0463	R1 = 0.0433, wR2 = 0.0732	R1 = 0.0412, wR2 = 0.0668	R1 = 0.0474, wR2 = 0.0930
R indices (all data)	R1 = 0.0197, wR2 = 0.0465	R1 = 0.0226, wR2 = 0.0541	R1 = 0.0336, wR2 = 0.0615	R1 = 0.0615, wR2 = 0.0499	R1 = 0.0718, wR2 = 0.0784	R1 = 0.0818, wR2 = 0.0743	R1 = 0.0849, wR2 = 0.0993
largest diff peak and hole, e Å ⁻³	0.668 and -0.545	0.843 and -0.827	1.493 and -0.836	1.038 and -0.957	0.420 and -0.430	0.681 and -0.470	1.043 and -0.937

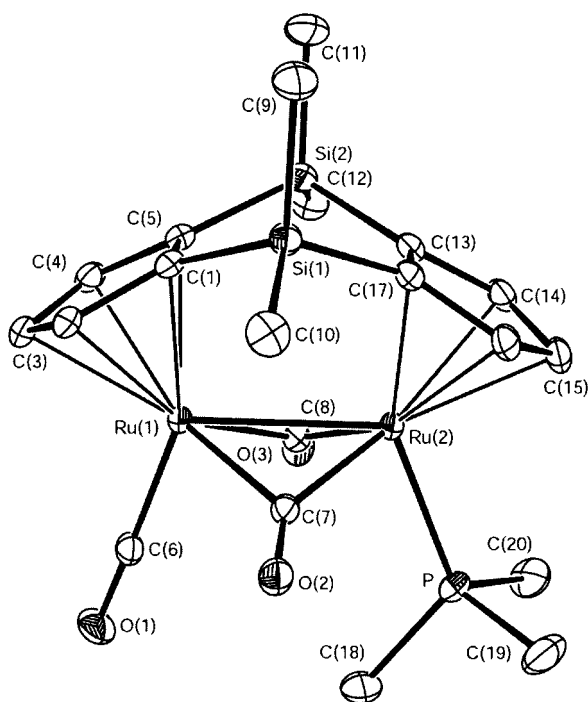
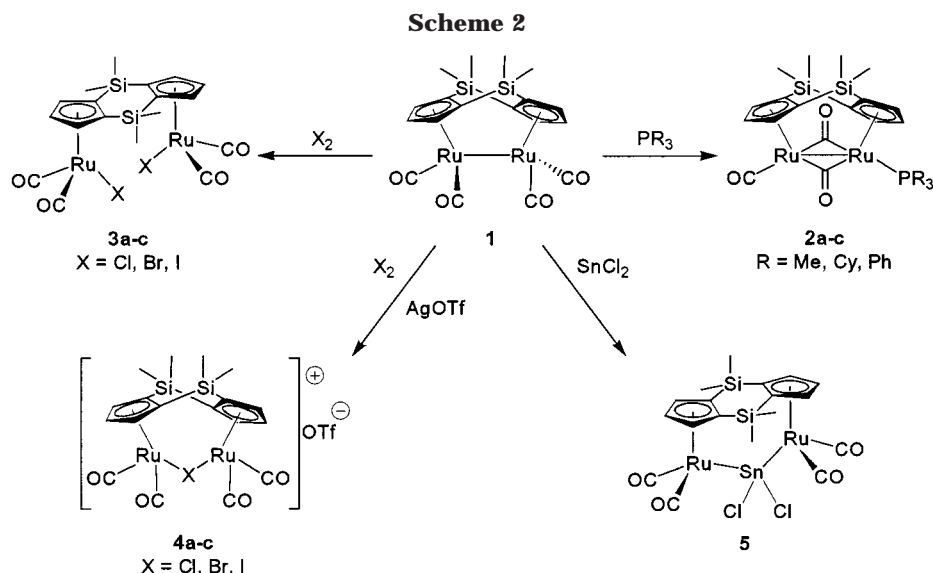


Figure 2. Thermal ellipsoid drawing of $\{(\eta^5\text{-C}_5\text{H}_3)_2(\text{SiMe}_2)_2\}\text{Ru}_2(\text{CO})(\mu\text{-CO})_2(\text{PMe}_3)$ (**2a**) showing the labeling scheme and 30% probability ellipsoids. Hydrogens are omitted for clarity. Selected bond distances (Å) and angles (deg) are as follows: Ru(1)–Ru(2), 2.6579(2); Ru(1)–C(6), 1.848(2); Ru(1)–C(7), 2.104(2); Ru(1)–C(8), 2.088(2); Ru(2)–C(7), 1.992(2); Ru(2)–C(8), 1.998(2); Ru(2)–P, 2.2770(6); Ru(1)–Cp(centroid), 1.936(2); Ru(2)–Cp(centroid), 1.910; $\angle\text{C}(6)\text{--Ru}(1)\text{--C}(7)$, 86.45(9); $\angle\text{C}(6)\text{--Ru}(1)\text{--C}(8)$, 86.96(9); $\angle\text{C}(7)\text{--Ru}(1)\text{--C}(8)$, 84.78(8); $\angle\text{P--Ru}(2)\text{--C}(7)$, 85.98(6); $\angle\text{P--Ru}(2)\text{--C}(8)$, 86.27(6); $\angle\text{C}(7)\text{--Ru}(2)\text{--C}(8)$, 90.20(8); $\angle\text{Ru}(1)\text{--Ru}(2)\text{--P}$, 111.833(17); $\angle\text{Ru}(2)\text{--Ru}(1)\text{--C}(6)$, 110.21(7); $\angle\text{Cp}(\text{centroid})\text{--Ru}(1)\text{--Ru}(2)\text{--Cp}(\text{centroid})$, 0.1; $\angle\text{C}(6)\text{--Ru}(1)\text{--Ru}(2)\text{--P}$, 0.5; $\angle\text{Cp--Cp}$ fold angle, 119.0.

the Ru(1)–C(7)–Ru(2) and Ru(1)–C(8)–Ru(2) planes (130.5°), compared to that found in $\text{Cp}_2\text{Ru}_2(\text{CO})(\mu\text{-CO})_2(\text{PMe}_3)$ (155.5°). The Ru(2)–C(7) and Ru(2)–C(8) distances (1.992(2), 1.998(2) Å) are shorter than the Ru(1)–C(7) and Ru(1)–C(8) distances (2.104(2), 2.088(2) Å), as expected for the more electron-rich Ru(2) center. There is no twist around the Ru–Ru bond, as indicated

by the torsion angles $\angle\text{Cp}(\text{centroid})\text{--Ru}(1)\text{--Ru}(2)\text{--Cp}(\text{centroid})$ (0.1°) and $\angle\text{C}(6)\text{--Ru}(1)\text{--Ru}(2)\text{--P}$ (0.5°).

Reactions of $\{(\eta^5\text{-C}_5\text{H}_3)_2(\text{SiMe}_2)_2\}\text{Ru}_2(\text{CO})_4$ (1**) with Halogens. Synthesis of $\{(\eta^5\text{-C}_5\text{H}_3)_2(\text{SiMe}_2)_2\}\text{Ru}_2(\text{CO})_4(\mu\text{-X})_2$ (**3a–c**) and $[\{(\eta^5\text{-C}_5\text{H}_3)_2(\text{SiMe}_2)_2\}\text{Ru}_2(\text{CO})_4(\mu\text{-X})]^+\text{TfO}^-$ (**4a–c**).** It is well-known⁹ that the dimeric $\text{Cp}'_2\text{M}_2(\text{CO})_4$ (M = Fe, Ru, Os) complexes react with halogens (X_2) to give metal(II) halide carbonyl complexes $\text{Cp}'\text{M}(\text{CO})_2\text{X}$. Similarly, complex **1** reacts with X_2 (X = Cl, Br, I) in CH_2Cl_2 at room temperature to give complexes **3a–c** (Scheme 2) (71–85% yield), which were isolated as yellow air-stable solids. Their IR spectra in hexanes solutions show the expected two strong $\nu(\text{CO})$ absorptions in the ranges 2052–2060 and 2000–2006 cm^{-1} . Their ^1H NMR spectra at room temperature show a doublet and a triplet in the range δ 5.21–5.49 for the protons of each cyclopentadienyl ring, consistent with an AB_2 spin system. This pattern remains unchanged at low temperature (–50 °C). An X-ray structural determination of **3c** shows (Figure 3, Table 1) that the asymmetric unit contains *three* different molecules. In each of these molecules the Ru atoms exhibit a three-legged piano-stool geometry. The most interesting feature of the structure is the almost flat conformation of the $(\eta^5\text{-C}_5\text{H}_3)_2(\text{SiMe}_2)_2$ ligand ($\angle\text{Cp--Cp}$ fold angle 175.9°), which is consistent with the long Ru–Ru nonbonding distance (4.9762 Å). The cyclopentadienyl rings of the bridging ligand are slightly twisted with respect to each other, which is evident in the torsion angle $\angle\text{Cp}(\text{centroid})\text{--Ru}(1)\text{--Ru}(2)\text{--Cp}(\text{centroid})$ (5.3°). This twist may reflect steric repulsions between the cisoid $\text{Ru}(\text{CO})_2\text{I}$ units.

The halide-bridged cationic complexes $\{(\eta^5\text{-C}_5\text{H}_3)_2(\text{SiMe}_2)_2\}\text{Ru}_2(\text{CO})_4(\mu\text{-X})_2^+$ can be isolated from aromatic solvents as intermediates from reactions of $\text{Cp}'_2\text{M}_2(\text{CO})_4$ and halogens (X_2) in the presence of large counterions.¹⁰ Although we did not observe similar intermediates in the reactions of **1** with halogens, the corresponding cationic, halide-bridged complexes $[\{(\eta^5\text{-C}_5\text{H}_3)_2(\text{SiMe}_2)_2\}\text{Ru}_2(\text{CO})_4(\mu\text{-X})]^+\text{TfO}^-$ (**4a–c**) were readily accessible as air-stable

(9) Bennett, M. A.; Bruce, M. I.; Matheson, T. W. In *Comprehensive Organometallic Chemistry*; Wilkinson, G., Stone, F. G. A., Abel, E. W., Eds., Pergamon Press: Oxford, New York, 1982; Vol. 4, p 821.

(10) Haines, R. J.; duPreez, A. L. C. *J. Chem. Soc., Dalton Trans.* **1972**, 944.

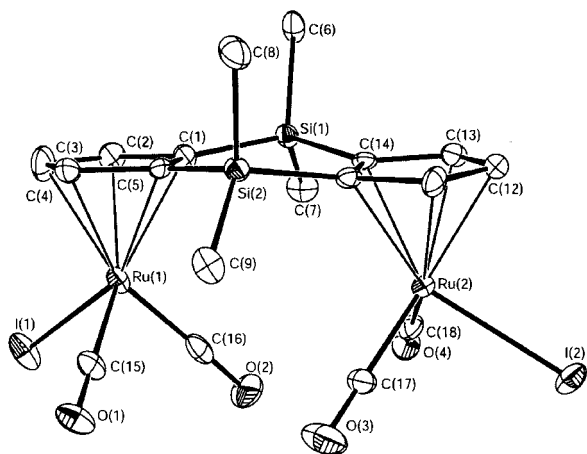


Figure 3. Thermal ellipsoid drawing of $\{(\eta^5\text{-C}_5\text{H}_3)_2(\text{SiMe}_2)_2\}\text{Ru}_2(\text{CO})_4(\text{I})_2$ (**3c**) showing the labeling scheme and 30% probability ellipsoids; hydrogens are omitted for clarity. Selected bond distances (Å) and angles (deg) are as follows: Ru(1)–Ru(2), 4.9762; Ru(1)–I(1), 2.7070(7); Ru(1)–C(15), 1.878(7); Ru(1)–C(16), 1.882(9); Ru(1)–Cp(centroid), 1.883; Ru(2)–Cp(centroid), 1.872; \angle I(1)–Ru(1)–C(15), 90.7(2); \angle I(1)–Ru(1)–C(16), 85.7(4); \angle C(16)–Ru(1)–C(15), 88.2(3); \angle Cp(centroid)–Ru(1)–Ru(2)–Cp(centroid), 5.3; \angle Cp–Cp fold angle, 175.9.

solids (51–85% yield) by the reaction of complex **1** and X_2 ($\text{X} = \text{Cl}, \text{Br}, \text{I}$) in the presence of a large excess of AgTfO at room temperature. It is worth mentioning that, in contrast to the corresponding monolinked ($\{(\eta^5\text{-C}_5\text{H}_4)_2(\text{SiMe}_2)\}\text{Ru}_2(\text{CO})_4(\mu\text{-X})\}^+$)¹¹ and nonlinked ($\{\text{Cp}_2\text{-Ru}_2(\text{CO})_4(\mu\text{-X})\}^+$)⁹ Ru complexes, compounds **4a–c** do not react with an excess of AgTfO further in acetonitrile to give the dicationic complexes $\{[(\eta^5\text{-C}_5\text{H}_3)_2(\text{SiMe}_2)_2]\text{Ru}_2(\text{CO})_4(\text{MeCN})_2\}^{2+}$; this indicates an unusual stability of the bridging halide in the complexes with the doubly linked $(\eta^5\text{-C}_5\text{H}_3)_2(\text{SiMe}_2)_2$ ligand. The ^1H NMR spectra of **4a–c** show a doublet and a triplet (AB_2 spin system) for the equivalent cyclopentadienyl rings and two singlets for the methyl groups in the SiMe_2 groups of the ligand, as expected for a symmetrical structure.

Insertion of SnCl_2 into the Ru–Ru Bond in **1.** Stannous chloride (SnCl_2) has been reported¹² to react with $\text{Cp}_2\text{M}_2(\text{CO})_4$ ($\text{M} = \text{Fe}, \text{Ru}$) complexes to give the products $\text{Cp}_2\text{M}_2(\text{CO})_4(\mu\text{-SnCl}_2)$, in which the Sn inserts into the M–M bond. When **1** and SnCl_2 are refluxed in THF for 30 h, $\{(\eta^5\text{-C}_5\text{H}_3)_2(\text{SiMe}_2)_2\}\text{Ru}_2(\text{CO})_4(\mu\text{-SnCl}_2)$ (**5**) is obtained in 74% yield as an air-stable yellow crystalline solid. The ^1H NMR spectrum of **5** shows a doublet and a triplet at δ 5.58 and 5.64 for the protons in the equivalent cyclopentadienyl rings and two singlets for the different CH_3 protons in the SiMe_2 groups. The IR spectrum exhibits three strong $\nu(\text{CO})$ bands in the 1986–2038 cm^{-1} region. A single-crystal X-ray structural determination (Figure 4, Table 1) of **5** shows that *three* different molecules are present in the asymmetric unit. In all three molecules, each Ru has a three-legged piano-stool structure. The Ru–Sn bond distances are almost identical in all three molecules (2.6034(4)–2.6066(4) Å). The presence of the bridging SnCl_2 ligand leads to an Ru–Ru distance of 4.625 Å, much longer

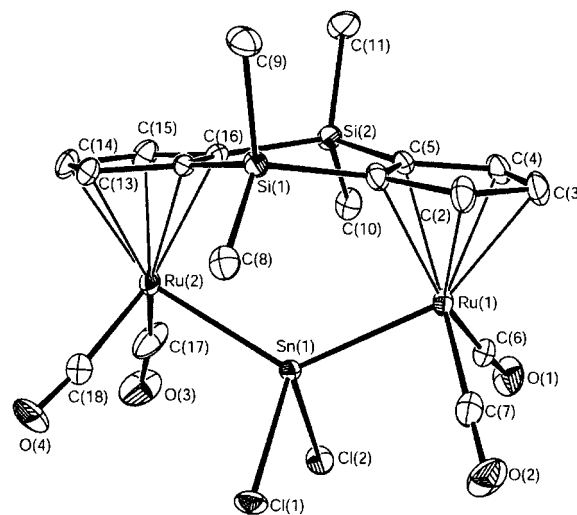


Figure 4. Thermal ellipsoid drawing of $\{(\eta^5\text{-C}_5\text{H}_3)_2(\text{SiMe}_2)_2\}(\text{CO})_4(\mu\text{-SnCl}_2)$ (**5**) showing the labeling scheme and 30% probability ellipsoids. Hydrogens are omitted for clarity. Selected bond distances (Å) and angles (deg) are as follows: Ru(1)–Ru(2), 4.625; Ru(1)–C(6), 1.874(4); Ru(1)–C(7), 1.887(4); Ru(1)–Sn(1), 2.6066(4); Ru(2)–C(17), 1.875(4); Ru(2)–C(18), 1.864(5); Ru(2)–Sn(1), 2.6034(4); Sn(1)–Cl(1), 2.4497(9); Sn(1)–Cl(2), 2.4465(9); Ru(1)–Cp(centroid), 1.895; Ru(2)–Cp(centroid), 1.887; \angle C(7)–Ru(1)–C(6), 92.68(17); \angle C(6)–Ru(1)–Sn(1), 87.02(12); \angle C(7)–Ru(1)–Sn(1), 88.29(12); \angle Cl(1)–Sn(1)–Cl(2), 92.73(3); \angle Ru(1)–Sn(1)–Ru(2), 125.162(13); \angle Ru(1)–Sn(1)–Cl(1), 109.24(3); \angle Cp(centroid)–Ru(1)–Ru(2)–Cp(centroid), 3.1; \angle Cp–Cp fold angle, 171.1.

than that (2.8180(3) Å) in complex **1** but shorter than that (4.9762 Å) in **3c**. The long Ru–Ru distance in **5** leads to a Cp–Cp fold angle that is significantly larger (171.1°) than that (122.86°) in complex **1** but smaller than that (175.9°) in **3c**. The twist around the Ru–Ru axis is minimal, which is reflected in the small \angle Cp(centroid)–Ru(1)–Ru(2)–Cp(centroid) torsion angle (3.1°).

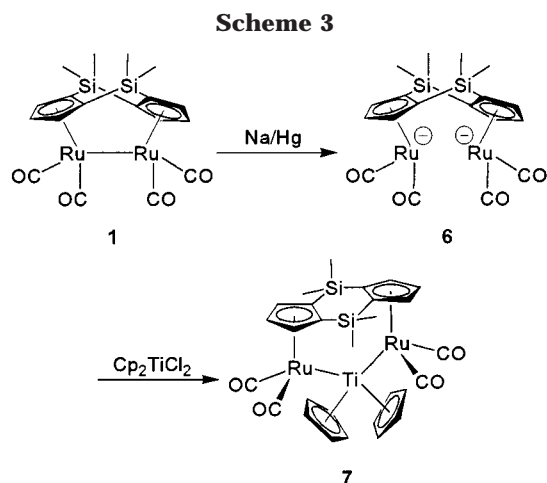
Generation of $[(\eta^5\text{-C}_5\text{H}_3)_2(\text{SiMe}_2)_2]\text{Ru}_2(\text{CO})_4\}^{2-}$ (6**) and Synthesis of $\{(\eta^5\text{-C}_5\text{H}_3)_2(\text{SiMe}_2)_2\}\text{Ru}_2(\text{CO})_4\{\mu\text{-Ti}(\eta^5\text{-C}_5\text{H}_5)_2\}$ (**7**).** It is known⁹ that the dimeric $\text{Cp}'_2\text{Ru}_2(\text{CO})_4$ complexes react with Na amalgam to give the anionic complexes $\text{Cp}'\text{Ru}(\text{CO})_2^-$, which can react with various electrophiles (MeI, Me_3SnCl , etc.). The related anionic complex $\{(\eta^5\text{-C}_5\text{H}_3)_2(\text{SiMe}_2)_2\}\text{Ru}_2(\text{CO})_4\}^{2-}$ (**6**) was generated in situ from the reaction of **1** with Na/Hg but was too reactive to be isolated. However, **6** reacts with 1 equiv of $(\eta^5\text{-C}_5\text{H}_5)_2\text{TiCl}_2$ at room temperature in THF to give $\{(\eta^5\text{-C}_5\text{H}_3)_2(\text{SiMe}_2)_2\}\text{Ru}_2(\text{CO})_4\{\mu\text{-Ti}(\eta^5\text{-C}_5\text{H}_5)_2\}$ (**7**) (Scheme 3; 53%), which was isolated as extremely moisture-sensitive pale yellow crystals. The $\nu(\text{CO})$ bands of **7** at 1938 and 1876 cm^{-1} are shifted to lower energy from the corresponding bands (2025 and 1967 cm^{-1}) of **1**, as expected for complexes of this type: for example, $(\eta^5\text{-C}_5\text{H}_5)_2\text{Ru}_2(\text{CO})_4\{\mu\text{-Zr}(\eta^5\text{-C}_5\text{H}_5)_2\}$.¹³ The two Ti–Cp groups are equivalent in the ^1H NMR spectrum. Unfortunately, we were unable to obtain X-ray-quality crystals of **7**.

Reaction of $\{(\eta^5\text{-C}_5\text{H}_3)_2(\text{SiMe}_2)_2\}\text{Ru}_2(\text{CO})_4$ (1**) with Diphenylacetylene. Synthesis of $\{(\eta^5\text{-C}_5\text{H}_3)_2(\text{SiMe}_2)_2\}\text{Ru}_2(\text{CO})_2(\mu\text{-CO})\{\eta^1\text{-}\eta^1\text{-}\mu_2\text{-C}(\text{Ph})\text{C}(\text{Ph})\}$ (**8**), $\{(\eta^5\text{-C}_5\text{H}_3)_2(\text{SiMe}_2)_2\}\text{Ru}_2(\text{CO})\{\eta^2\text{-}\eta^4\text{-}\mu_2\text{-C}(\text{Ph})\text{C}(\text{Ph})\text{C}(\text{Ph})\}$**

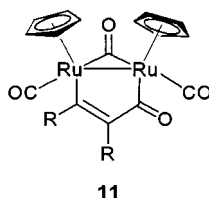
(11) Fröhlich, R.; Gimeno, J.; González-Cueva, M.; Lastra, E.; Borge, J.; García-Granda, S. *Organometallics* **1999**, *18*, 3008.

(12) Zhang, Y.; Xu, S.; Tian, G.; Zhang, W.; Zhou, X. *J. Organomet. Chem.* **1997**, *544*, 43 and references therein.

(13) Casey, C. P.; Jordan, R. F.; Rheingold, A. L. *Organometallics* **1984**, *3*, 504.



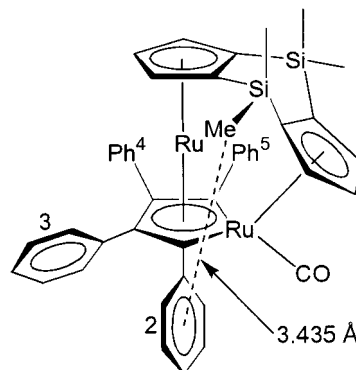
C(Ph) (**9**), and $\{(\eta^5\text{-C}_5\text{H}_3)_2(\text{SiMe}_2)_2\}\text{Ru}_2(\text{CO})\{\eta^2:\eta^4\text{-}\mu_2\text{-C(=O)C(Ph)C(Ph)C(Ph)C(Ph)}\}$ (**10**). Ultraviolet irradiation of a benzene solution containing **1** and 4 equiv of diphenylacetylene for 25 h produces the bimetallic Ru complexes **8–10** (Scheme 4), which were successfully separated by chromatography. There was no evidence for the formation of a $\{(\eta^5\text{-C}_5\text{H}_3)_2(\text{SiMe}_2)_2\}$ -based diruthenacyclopentenone analogous to **11**, which is obtained upon photolysis of $\text{Cp}_2\text{Ru}_2(\text{CO})_4$ in the presence of alkynes (e.g. mono- and diphenylacetylene).¹⁴



Complex **8**, which was obtained as dark red, air-sensitive crystals, was identified by characteristic patterns in its ¹H NMR and IR spectra, which are similar to those of the known analogous complexes $\{(\eta^5\text{-C}_5\text{H}_4)_2(\text{CMe}_2)\}\text{Ru}_2(\text{CO})_2(\mu\text{-CO})\{\eta^1:\eta^1\text{-}\mu_2\text{-C(Ph)C(Ph)}\}$ ¹⁵ and $\{(\eta^5\text{-C}_5\text{H}_4)_2\}\text{Ru}_2(\text{CO})_2(\mu\text{-CO})\{\eta^1:\eta^1\text{-}\mu_2\text{-CHCH}\}$.⁶ In the ¹H NMR spectrum, the presence of three signals in the cyclopentadienyl region and four signals corresponding to the Si(CH₃)₂ methyl groups are consistent with the proposed structure of **8**. Its IR spectrum ($\nu(\text{CO})$: 1983, 1935, and 1753 cm⁻¹) indicates the presence of both terminal and bridging CO ligands.

Complex **9** is an air-stable orange crystalline solid that is soluble in benzene and CH₂Cl₂ and moderately soluble in nonpolar solvents (hexanes). The IR spectrum of **9** in hexanes shows only one sharp $\nu(\text{CO})$ band at 1969 cm⁻¹, which corresponds to the terminal CO ligand coordinated to one of the Ru atoms. The ¹H NMR spectrum of **9** exhibits resonances for the inequivalent Cp rings (each displays a unique AB₂ splitting pattern) and two signals for the Si(CH₃)₂ methyl groups at δ

–0.62 and 0.36. The δ –0.62 signal is approximately 0.7 ppm upfield from the typical Si(CH₃)₂ region and indicates a pronounced shielding of the equatorial methyl groups by the nearby phenyl rings. The X-ray structure of **9** (Figure 5, Table 1), which is discussed in more detail below, confirms a close nonbonding interaction (3.435 Å) between the SiMe₂ equatorial methyl groups and the π -systems of phenyl groups 2 and 5.



The variable-temperature ¹H NMR spectrum of **9** in CD₂Cl₂ in the aromatic region is shown in Figure 6. At –50 °C, the spectrum consists of 10 (δ 6.42, 6.58, 6.65, 6.77, 6.83, 6.88, 7.03, 7.09, 7.12, 7.62) well-resolved resonances of equal intensity. As the temperature is increased to –20 °C, 4 of the 10 resonances (δ 6.58, 6.77, 7.09, 7.62) coalesce to a single broad resonance, which is almost indistinguishable from the baseline. At +25 °C a new broad signal is observed at δ 7.25 ppm and the signal at δ 6.88 ppm gains intensity and broadens, while the other 5 resonances at δ 7.12, 7.03, 6.83, 6.65, and 6.42 remain virtually unchanged. We can assign the latter set of five resonances to the equivalent phenyl rings 3 and 4, which are not fluxional with respect to rotation around the C(3 or 4)–phenyl bond in the –50 to +25 °C temperature range. A ¹H–¹H COSY experiment demonstrates the mutual coupling of these 5 signals. Broad resonances at δ 7.25 and 6.88 ppm (+25 °C) are assigned to the ortho and meta protons of the equivalent phenyl groups 2 and 5, indicating fluxionality at room temperature on the NMR time scale. The simplest explanation for the temperature-dependent appearance of phenyl groups 2 and 5 in the ¹H NMR spectra is the lack of free rotation around the C(2 or 5)–phenyl bond at –50 °C, when five signals are observed. An NOE experiment indicates the presence of a weak through-space interaction between the equatorial SiMe₂ methyl groups and phenyl rings 2 and 5. As the temperature is increased to +25 °C, this rotational motion becomes semirestricted. Further sharpening of resonances at δ 7.25 and 6.88 ppm in the ¹H NMR spectra was observed at temperatures up to +50 °C.

In the molecular structure of **9** (Figure 5, Table 1), there is an approximate (noncrystallographic) mirror plane containing Ru(1), Ru(2), and the centroids of the two Cp rings. The Ru(1)–Ru(2) distance is 2.6221(6) Å, corresponding to a single Ru–Ru bond. The two ruthenium atoms are bridged by a $\{\eta^2:\eta^4\text{-}\mu_2\text{-C(Ph)C(Ph)C(Ph)C(Ph)}\}$ fragment, the ends of which are σ -bonded to Ru(1), forming a metallacyclopentadiene ring. The Ru(1)–C(2) and Ru(1)–C(5) distances of 2.100(4) and 2.096(4) Å are consistent with Ru–C single bonds, as

(14) (a) Albers, M. O.; Robinson, D. J.; Singleton, E. *Coord. Chem. Rev.* **1987**, *79*, 1. (b) Davies, D. L.; Dyke, A. F.; Knox, S. A. R.; Morris, M. J. *J. Organomet. Chem.* **1981**, *215*, C30

(15) (a) Nelson, G. O.; Wright, M. E. *J. Organomet. Chem.* **1981**, *206*, C21. (b) Knox, S. A. R.; Macpherson, K. A.; Orpen, A. G.; Rendle, M. C. *J. Chem. Soc., Dalton Trans.* **1989**, 1807.

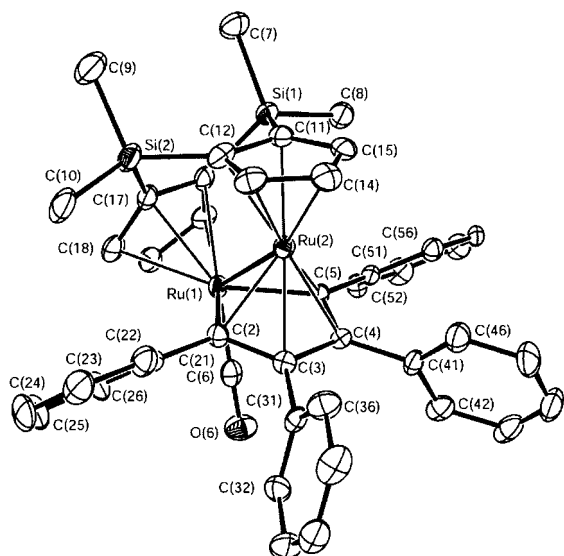
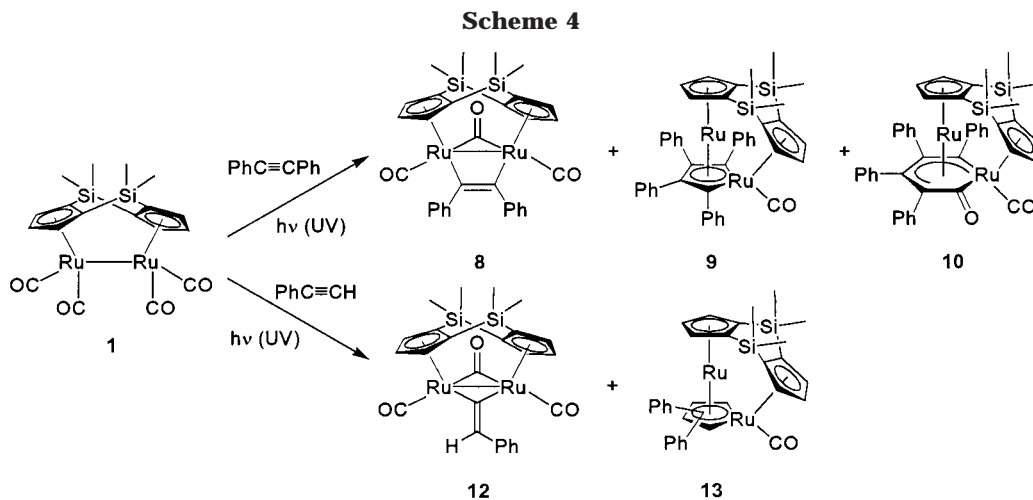


Figure 5. Thermal ellipsoid drawing of $\{(\eta^5\text{-C}_5\text{H}_3)_2(\text{Si-Me}_2)_2\}\text{Ru}_2(\text{CO})\{\eta^2:\eta^4\text{-}\mu_2\text{-C}(\text{Ph})\text{C}(\text{Ph})\text{C}(\text{Ph})\text{C}(\text{Ph})\}$ (**9**) showing the labeling scheme and 30% probability ellipsoids. Hydrogens are omitted for clarity. Selected bond distances (Å) and angles (deg) are as follows: Ru(1)–Ru(2), 2.6221(6); Ru(1)–C(6), 1.845(6); Ru(1)–C(5), 2.096(4); Ru(1)–C(2), 2.100(4); C(2)–C(3), 1.428(6); C(3)–C(4), 1.438(6); C(4)–C(5), 1.424(6); Ru(1)–Cp(centroid), 1.936; Ru(2)–Cp(centroid), 1.829; Ru(2)–ruthenacyclopentadiene(Ru(1), C(2)–C(5))(centroid), 1.753; C(8)–phenyl(C51–C(56))(centroid), 3.435; $\angle\text{C(6)–Ru(1)–C(5)}$, 80.8(2); $\angle\text{C(6)–Ru(1)–C(2)}$, 79.9(2); $\angle\text{C(5)–Ru(1)–C(2)}$, 78.05(17); $\angle\text{Cp(centroid)–Ru(2)–ruthenacyclopentadiene(Ru(1), C(2)–C(5))(centroid)}$, 172.17; $\angle\text{Cp–Cp fold angle}$, 118.83.

are the Ru(2)–C(2) and Ru(2)–C(5) lengths of 2.133(5) and 2.130(4) Å. The Ru(1)–C(2)–C(3)–C(4)–C(5) ring may be viewed as being π -bound to Ru(2), but this bonding does not result in the geometry observed for other related dinuclear complexes, such as $(\eta^2\text{-MeCC-Me})\text{W}_2(\text{OPr}^i)_5(\mu_2\text{-OPr}^i)(\eta^2:\eta^4\text{-}\mu_2\text{-C}_4\text{Me}_4)$, which contains planar rings.¹⁶ Instead, the Ru(1)–C(2)–C(3)–C(4)–C(5) ring is puckered, with Ru(1) lying 0.41 Å out of the least-squares plane defined by carbon atoms C(2)–C(5) and away from Ru(2). The angle between the C(2)–C(3)–C(4)–C(5) and Ru(1)–C(2)–C(5) planes is 166.78°.

(16) (a) Chisholm, M. H.; Hoffman, D. M.; Huffman, J. C. *J. Am. Chem. Soc.* **1984**, *106*, 6806. (b) Bruce, M. I.; Matison, J. G.; Skelton, B. W.; White, A. H. *J. Organomet. Chem.* **1983**, *251*, 249.

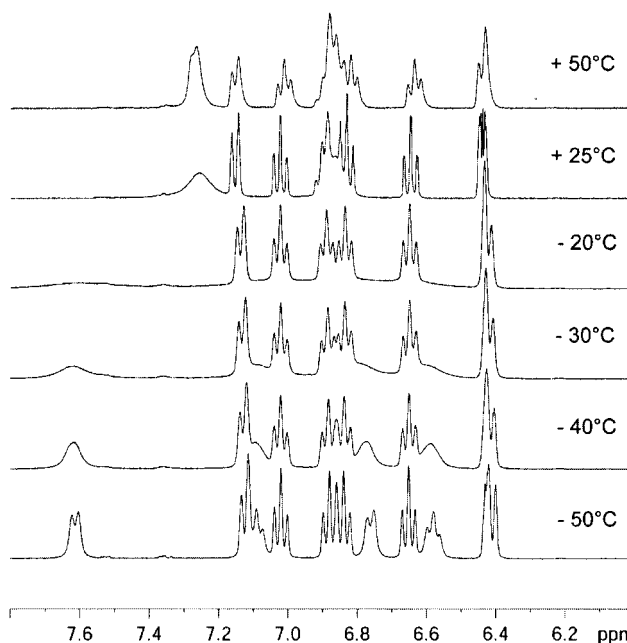


Figure 6. Variable-temperature ^1H NMR spectra in the aromatic region of **9** in CD_2Cl_2 at 400 MHz.

The mean plane of the C(2)–C(3)–C(4)–C(5) fragment is nearly parallel ($\angle\text{Cp(centroid)–Ru(2)–ruthenacyclopentadiene(Ru(1), C(2)–C(5))(centroid)} = 172.17^\circ$) to the plane of the cyclopentadienyl ring bound to Ru(2), giving Ru(2) a pseudo-metallocene coordination environment. The phenyl groups C(31)–C(36) and C(41)–C(46) are almost orthogonal to the C(2)–C(3)–C(4)–C(5) plane (76.4 and 80.6°), while the phenyl groups C(21)–C(26) and C(51)–C(56) have tilt angles of 50.7 and 51.5°, due to close through-space interactions with the equatorial methyl groups of the SiMe₂ linkers. Structural features of **9** are similar to those of other dinuclear ruthenacyclopentadiene complexes such as $(\eta^5\text{-C}_5\text{Me}_5)_2\text{Cl}_2\text{Ru}_2(\eta^2:\eta^4\text{-}\mu_2\text{-C}_4\text{H}_4)(\eta^5\text{-C}_5\text{Me}_5)$,¹⁷ $(\eta^5\text{-C}_5\text{Me}_5)(\text{CO})\text{Ru}(\eta^2:\eta^4\text{-}\mu_2\text{-C}(\text{ToI})\text{CHC}(\text{ToI})\text{CH})\text{Co}(\text{CO})_2$,¹⁷ and $[(\eta^5\text{-C}_5\text{Me}_5)(\text{MeCN})\text{Ru}(\eta^4\text{-}\mu_2\text{-C}_4\text{H}_2\text{Ph}_2)\text{Ru}(\eta^5\text{-C}_5\text{Me}_5)](\text{CF}_3\text{SO}_3)$.¹⁹

(17) Campion, B. K.; Heyn, R. H.; Tilley, T. D. *Organometallics* **1990**, *9*, 1106.

(18) Matsuzaka, H.; Ichikawa, K.; Ishioka, T.; Sato, H.; Okubo, T.; Ishii, T.; Yamashita, M.; Kondo, M.; Kitagawa, S. *J. Organomet. Chem.* **2000**, *596*, 121.

(19) He, X. D.; Chaudret, B.; Dahan, F.; Huang, Y.-S. *Organometallics* **1991**, *10*, 970.

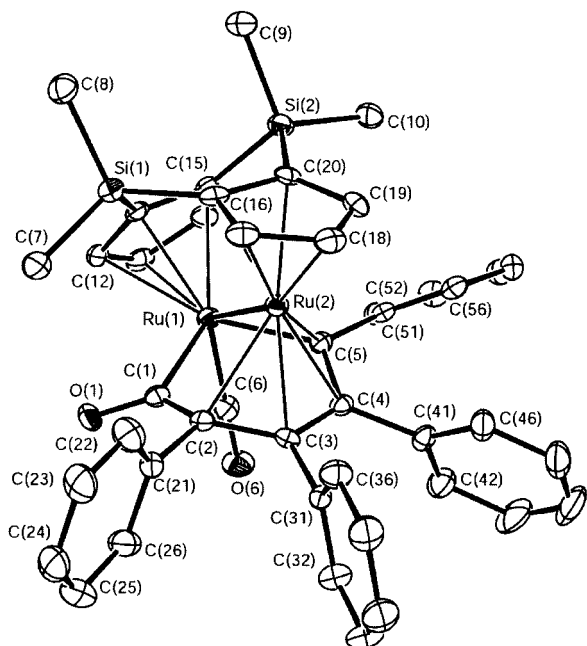


Figure 7. Thermal ellipsoid drawing of $\{(\eta^5\text{-C}_5\text{H}_5)_2(\text{SiMe}_2)_2\text{Ru}_2(\text{CO})\{\eta^2:\eta^4\text{-}\mu_2\text{-C(=O)C(Ph)C(Ph)C(Ph)C(Ph)}\}$ (**10**) showing the labeling scheme and 30% probability ellipsoids. Hydrogens are omitted for clarity. Selected bond distances (Å) and angles (deg) are as follows: Ru(1)–Ru(2), 2.7118(6); Ru(1)–C(6), 1.856(5); Ru(1)–C(5), 2.083(4); Ru(1)–C(1), 2.029(4); C(1)–O(1), 1.219(5); C(1)–C(2), 1.482(6); C(2)–C(3), 1.444(5); C(3)–C(4), 1.431(5); C(4)–C(5), 1.431(5); Ru(2)–C(1), 2.796; Ru(2)–C(2), 2.274(4); Ru(2)–C(3), 2.211(4); Ru(2)–C(4), 2.226(4); Ru(2)–C(5), 2.110(4); Ru(1)–Cp(centroid), 1.967; Ru(2)–Cp(centroid), 1.848; Ru(2)–ruthenacyclopentadiene(Ru(1),C(2)–C(5))(centroid), 1.769; C(10)–phenyl(C51–C56)(centroid), 3.476; $\angle\text{C(6)–Ru(1)–C(5)}$, 78.47(17); $\angle\text{C(6)–Ru(1)–C(1)}$, 78.54(17); $\angle\text{C(5)–Ru(1)–C(1)}$, 95.00(17); $\angle\text{Cp(centroid)–Ru(2)–ruthenacyclopentadiene(Ru(1),C(2)–C(5))(centroid)}$, 174.27; $\angle\text{Cp–Cp}$ fold angle, 123.53.

Spectroscopic and structural features of $\{(\eta^5\text{-C}_5\text{H}_5)_2(\text{SiMe}_2)_2\text{Ru}_2(\text{CO})\{\eta^2:\eta^4\text{-}\mu_2\text{-C(=O)C(Ph)C(Ph)C(Ph)C(Ph)}\}$ (**10**) are similar to those of complex **9**. Compound **10** differs from **9** only by the insertion of a CO group into a Ru(1)–C(2 or 5) bond of **9**. This leads to the lack of a mirror plane, which was present in complex **9**. As a result of the lower symmetry, the ^1H NMR spectrum of **10** exhibits resonances for the inequivalent Cp rings (each displays a unique ABC splitting pattern) and four signals for the $\text{Si}(\text{CH}_3)_2$ methyl groups at δ –1.00, 0.31, 0.36, and 0.57. The upfield signal indicates shielding of an equatorial methyl group by a nearby phenyl ring. The X-ray structure of **10** (Figure 7, Table 1) supports this close nonbonding interaction (3.476 Å) between the equatorial methyl C(10) and the plane of phenyl ring C(51)–C(56). The η^5 binding mode of the ruthenacyclohexadienone fragment to Ru(2) is supported by a long C(1)–C(2) bond (1.482(6) Å) compared to the C–C bonds in the delocalized C(2)–C(3)–C(4)–C(5) (1.444(5), 1.431(5), 1.431(5) Å) π -system and a nonbonding Ru(2)–C(1) distance (2.796 Å). The conformation of the ruthenacyclohexadienone Ru(1)–C(1)–C(2)–C(3)–C(4)–C(5) ring (Figure 8) cannot be described simply, because of significant out-of-plane deviations of each atom; the smallest dihedral angle in the Ru(1)–C(1)–C(2)–C(3)–C(4)–C(5) ring is $\angle\text{C(2)–C(3)–C(4)–C(5)}$ (10.3°). The

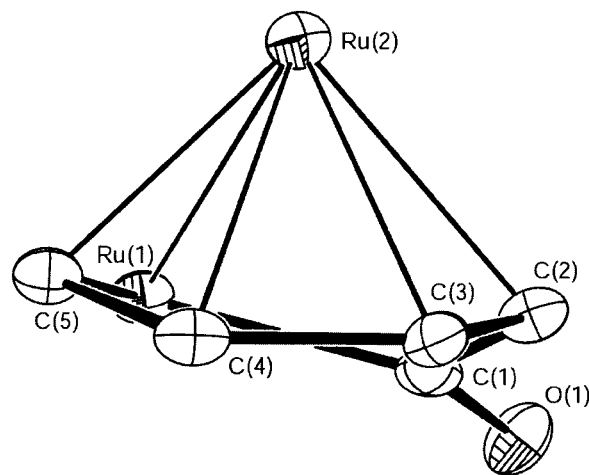


Figure 8. Structure of the core of $\{(\eta^5\text{-C}_5\text{H}_5)_2(\text{SiMe}_2)_2\text{Ru}_2(\text{CO})\{\eta^2:\eta^4\text{-}\mu_2\text{-C(=O)C(Ph)C(Ph)C(Ph)C(Ph)}\}$ (**10**).

IR spectrum of **10** in hexanes shows one sharp CO band at 1973 cm^{-1} , which corresponds to the terminal CO ligand coordinated to Ru(1), and a weak broad band at 1601 cm^{-1} , which may be assigned to the acyl CO group in the ruthenacyclohexadienone fragment.

Reaction of $\{(\eta^5\text{-C}_5\text{H}_5)_2(\text{SiMe}_2)_2\text{Ru}_2(\text{CO})_4$ (1**) with Phenylacetylene. Synthesis of $\{(\eta^5\text{-C}_5\text{H}_5)_2(\text{SiMe}_2)_2\text{Ru}_2(\text{CO})_2(\mu\text{-CO})(\mu\text{-C=CHPh})$ (**12**) and $\{(\eta^5\text{-C}_5\text{H}_5)_2(\text{SiMe}_2)_2\text{Ru}_2(\text{CO})\{\eta^2:\eta^4\text{-}\mu_2\text{-C(H)C(Ph)C(H)C(Ph)}\}$ (Mixture of Isomers) (**13**).** Ultraviolet irradiation of a solution containing **1** and 4 equiv of phenylacetylene (Scheme 4) in benzene solvent yields a mixture of products, which were identified as complexes **12** and **13** on the basis of spectral evidence. In contrast, ultraviolet irradiation of $\text{Cp}_2\text{Ru}_2(\text{CO})_4$ and phenylacetylene gives exclusively a complex of type **11** (R, R = H, Ph), which undergoes thermal (110 °C, toluene) rearrangement to the bridging vinylidene complex $\text{Cp}_2\text{Ru}_2(\text{CO})_2(\mu\text{-CO})(\mu\text{-C=CHPh})$.²⁰ The structure of **12** (Figure 9, Table 1) was conclusively established by an X-ray crystallographic analysis. The bridging $\mu\text{-C=CHPh}$ vinylidene ligand is planar ($\angle\text{Ru(1)–C(18)–C(19)–C(20)} = 0.2^\circ$) and bound almost symmetrically to both Ru atoms (Ru(1)–C(18) = 2.049(6) Å; Ru(2)–C(18) = 2.028(7) Å). As in complex **2a**, the Ru(1)–Ru(2) distance (2.6551(7) Å) is shorter compared to that (2.696(1) Å) in the nonlinked analogous complex $\text{Cp}_2\text{Ru}_2(\text{CO})_2(\mu\text{-CO})(\mu\text{-C=CH}_2)$.²⁰ The Cp–Cp fold angle (118.5°) is smaller compared to the same parameter (122.86°) for **1**. In fact, the structures of **12** and **2a**, especially the geometries around the Ru atoms, are very similar.

In the ^1H NMR spectrum of **12**, the cyclopentadienyl hydrogens occur as six sets of well-resolved multiplets; in addition, there are four singlet methyl resonances for the SiMe_2 groups, which are consistent with the symmetry of the solid-state molecule and indicate the absence of rotation around the C(18)–C(19) bond of the vinylidene ligand. In the IR spectrum of **12**, bands for both terminal (2008, 1982 cm^{-1}) and bridging (1819 cm^{-1}) carbonyl absorptions are evident.

We were unable to obtain X-ray-quality crystals of **13**, due in part to the fact that this compound is formed as

(20) Colborn, R. E.; Davies, D. L.; Dyke, A. F.; Endesfelder, A.; Knox, S. A. R.; Orpen, A. G.; Plaas, D. *J. Chem. Soc., Dalton Trans.* **1983**, 2661.

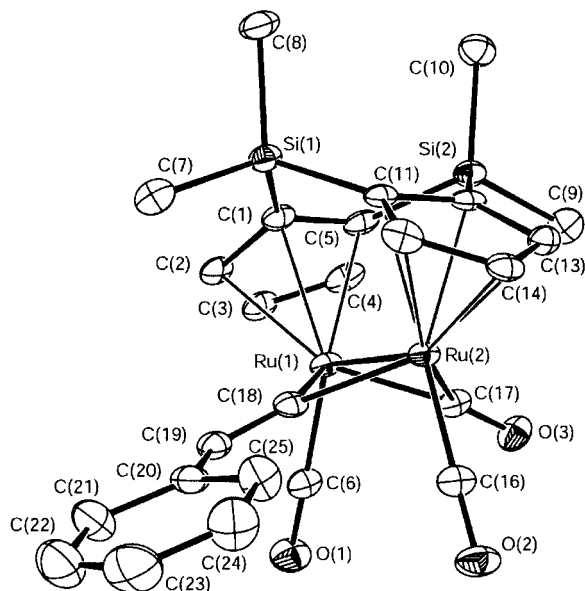


Figure 9. Thermal ellipsoid drawing of $\{(\eta^5\text{-C}_5\text{H}_3)_2(\text{SiMe}_2)_2\}\text{Ru}_2(\text{CO})_2(\mu\text{-CO})(\mu\text{-C}=\text{CHPh})$ (**12**) showing the labeling scheme and 30% probability ellipsoids. Hydrogens are omitted for clarity. Selected bond distances (Å) and angles (deg) are as follows: Ru(1)–Ru(2), 2.6551(7); Ru(1)–C(18), 2.049(6); Ru(2)–C(18), 2.028(7); C(18)–C(19), 1.312(8); C(19)–C(20), 1.475(8); Ru(1)–C(17), 2.023(7); Ru(2)–C(17), 2.060(6); Ru(1)–Cp(centroid), 1.919; Ru(2)–Cp(centroid), 1.918; $\angle\text{C(6)–Ru(1)–C(17)}$, 86.4(3); $\angle\text{C(6)–Ru(1)–C(18)}$, 83.8(2); $\angle\text{C(18)–Ru(1)–C(17)}$, 87.9(2); $\angle\text{C(16)–Ru(2)–C(17)}$, 83.8(2); $\angle\text{C(16)–Ru(2)–C(18)}$, 86.5(3); $\angle\text{C(18)–Ru(2)–C(17)}$, 87.4(2); $\angle\text{Ru(1)–Ru(2)–C(16)}$, 108.76(18); $\angle\text{Ru(2)–Ru(1)–C(6)}$, 108.78(19); $\angle\text{Ru(1)–C(18)–Ru(2)}$, 81.3(2); $\angle\text{Ru(1)–C(17)–Ru(2)}$, 81.1(3); $\angle\text{C(6)–Ru(1)–Ru(2)–C(16)}$, 0.2; $\angle\text{Cp(centroid)–Ru(1)–Ru(2)–Cp(centroid)}$, 0.9; $\angle\text{Cp–Cp fold angle}$, 118.5.

a mixture of three geometrical isomers. However, the patterns in the ^1H NMR and IR spectra are very similar to those of complex **9**, which suggests that **13** has the structure shown in Scheme 4. Attempts to isolate individual isomers of **13** by means of column chromatography were unsuccessful.

Conclusions

In summary, the dinuclear ruthenium complex $\{(\eta^5\text{-C}_5\text{H}_3)_2(\text{SiMe}_2)_2\}\text{Ru}_2(\text{CO})_4$ (**1**) is a precursor for the synthesis of a variety of new dinuclear ruthenium complexes, in which the bridging $(\eta^5\text{-C}_5\text{H}_3)_2(\text{SiMe}_2)_2$ ligand controls the geometry of the final product. This influence is particularly pronounced in the reactions of **1** and phenylacetylenes which give (Scheme 4) the unexpected complexes $\{(\eta^5\text{-C}_5\text{H}_3)_2(\text{SiMe}_2)_2\}\text{Ru}_2(\text{CO})\{\eta^2\text{-}\eta^4\text{-}\mu_2\text{-C(Ph)C(Ph)C(Ph)C(Ph)}\}$ (**9**), $\{(\eta^5\text{-C}_5\text{H}_3)_2(\text{SiMe}_2)_2\}\text{Ru}_2(\text{CO})\{\eta^2\text{-}\eta^4\text{-}\mu_2\text{-C(=O)C(Ph)C(Ph)C(Ph)C(Ph)}\}$ (**10**), and $\{(\eta^5\text{-C}_5\text{H}_3)_2(\text{SiMe}_2)_2\}\text{Ru}_2(\text{CO})\{\eta^2\text{-}\eta^4\text{-}\mu_2\text{-C(H)C(Ph)C(H)C(Ph)}\}$ (**13**) as major products. It is apparent that the $(\eta^5\text{-C}_5\text{H}_3)_2(\text{SiMe}_2)_2$ ligand stabilizes these unique structural motifs, which were not reported for nonlinked or monolinked dicyclopentadienyl Ru complexes. The steric properties and rigidity of the bridging $(\eta^5\text{-C}_5\text{H}_3)_2(\text{SiMe}_2)_2$ ligand are presumably also responsible for the unusual inertness of the bridging X^- ligand in the complexes $[\{(\eta^5\text{-C}_5\text{H}_3)_2(\text{SiMe}_2)_2\}\text{Ru}_2(\text{CO})_4(\mu\text{-X})]^+\text{TfO}^-$ ($\text{X} = \text{Cl, Br, I}$; **4a–c**) toward AgTfO . We have also demonstrated the

robustness of the $(\eta^5\text{-C}_5\text{H}_3)_2(\text{SiMe}_2)_2$ ligand, which remains unchanged in reactions of $\{(\eta^5\text{-C}_5\text{H}_3)_2(\text{SiMe}_2)_2\}\text{Ru}_2(\text{CO})_4$ (**1**) with phosphines, halogens, SnCl_2 , and Na/Hg to give a variety of new dinuclear doubly linked ruthenium(II) complexes.

Experimental Section

General Procedures. All reactions were performed under an argon atmosphere in reagent grade solvents, using standard Schlenk or drybox techniques.²¹ Hexanes, methylene chloride, and diethyl ether were purified by the Grubbs method prior to use.²² All other solvents were purified by published methods.²³ Chemicals were purchased from Aldrich Chemical Co., unless otherwise mentioned, or prepared by literature methods, as referenced below. Alumina (neutral, activity I, Aldrich) was degassed under vacuum for 12 h and treated with Ar-saturated water (7.5% w/w). ^1H and ^{13}C NMR spectra were recorded on a Bruker DRX-400 spectrometer using deuterated solvents as internal references. Solution infrared spectra were recorded on a Nicolet-560 spectrometer using NaCl cells with 0.1 mm spacers. Elemental analyses were performed on a Perkin-Elmer 2400 series II CHNS/O analyzer.

All photochemical reactions were carried out in 60 or 300 mL quartz Schlenk photolysis tubes fitted with a cold-finger condenser (which is immersed in the reaction solution) and using a Hanovia 450 W medium-pressure Hg lamp with a quartz jacket as the ultraviolet light source. The temperature of each reaction was controlled using an Isotemp 1013P refrigerated circulating bath (Fisher Scientific) with the circulating hoses connected to the cold finger.

Synthesis of $\{(\eta^5\text{-C}_5\text{H}_3)_2(\text{SiMe}_2)_2\}\text{Ru}_2(\text{CO})_3(\text{PMe}_3)$ (2a**).** To a solution of **1** (30 mg; 0.05 mmol) in decane (1 mL) in a thick-walled Pyrex tube was added PMe_3 (15 μL ; 0.15 mmol). The mixture was degassed, sealed under vacuum, heated to 200 °C for 24 h, and cooled to room temperature; the volatiles were removed under vacuum. The resulting orange-red residue was redissolved in CH_2Cl_2 (3 mL), and the solution was filtered through a short pad (3 cm) of alumina. Subsequent addition of hexanes (5 mL) and cooling (-20 °C) afforded crystalline **2a** (23 mg, 58%) as orange blades. ^1H NMR (400 MHz, CD_2Cl_2): δ 0.39 (s, 6 H, $\text{Si}(\text{CH}_3)_2$), 0.44 (s, 6 H, $\text{Si}(\text{CH}_3)_2$), 1.41 (d, $J_{\text{P-H}} = 9.6$ Hz, 9 H, $\text{P}(\text{CH}_3)_3$), 5.08 (d, $J = 2.4$ Hz, 2 H, Cp-H), 5.22 (m, 1 H, Cp-H), 5.39 (d, $J = 2.4$ Hz, 2 H, Cp-H), 5.84 (m, 1 H, Cp-H). ^{13}C NMR (100 MHz, CD_2Cl_2): δ -2.50, 3.96 ($\text{Si}(\text{CH}_3)_2$), 22.40 (d, $J_{\text{P-C}} = 30.5$ Hz, $\text{P}(\text{CH}_3)_3$), 86.67, 89.35, 91.41, 93.58, 95.66 (d, $J_{\text{P-C}} = 3.6$ Hz, Cp-C), 98.97 (Cp), 207.66, 220.28 (d, $J_{\text{P-C}} = 10.9$ Hz, CO). $^{31}\text{P}\{^1\text{H}\}$ NMR (161 MHz, CD_2Cl_2): δ 11.5 (s). IR (CH_2Cl_2): $\nu(\text{CO})$ (cm^{-1}) 1968 (vs), 1935 (m), 1907 (vs), 1733 (m). IR (hexanes): $\nu(\text{CO})$ (cm^{-1}) 1981 (vs), 1955 (w), 1917 (vs), 1905 (w), 1752 (w). IR (solid state, on PTFE tape): $\nu(\text{CO})$ (cm^{-1}) 1959 (vs), 1929 (s), 1901 (vs), 1881 (s), 1739 (s). Anal. Calcd for $\text{C}_{20}\text{H}_{27}\text{O}_3\text{PRu}_2\text{Si}_2$: C, 39.72; H, 4.50. Found: C, 39.38; H, 4.13.

Synthesis of $\{(\eta^5\text{-C}_5\text{H}_3)_2(\text{SiMe}_2)_2\}\text{Ru}_2(\text{CO})_3(\text{PCy}_3)$ (2b**).** A solution of **1** (30 mg, 0.053 mmol) in decane (1 mL) was reacted with PCy_3 (48 mg, 0.17 mmol) at 200 °C for 36 h, as in the preparation of **2a**. Two crystallizations of the resulting orange-red solid from CH_2Cl_2 –hexanes gave **2b** (29 mg, 74%) as red prisms. ^1H NMR (400 MHz, CD_2Cl_2): δ 0.46 (s, 6 H, $\text{Si}(\text{CH}_3)_2$), 0.66 (s, 6 H, $\text{Si}(\text{CH}_3)_2$), 1.56–2.04 (complex m, 33 H, $\text{P}(\text{C}_6\text{H}_{11})_3$), 5.10 (d, $J = 2.1$ Hz, 2 H, Cp-H), 5.56 (d, $J = 2.1$ Hz, 2 H, Cp-H), 5.79 (t, $J = 2.1$ Hz, 1 H, Cp-H), 5.90 (m, 1 H, Cp-H). $^{31}\text{P}\{^1\text{H}\}$ NMR (161 MHz, CD_2Cl_2): δ 49 (s). IR (CH_2 -

(21) Errington, R. J. *Advanced Practical Inorganic and Metalorganic Chemistry*, 1st ed.; Chapman & Hall: New York, 1997.

(22) Pangborn, A. B.; Giardello, M. A.; Grubbs, R. H.; Rosen, R. K.; Timmers, F. J. *Organometallics* **1996**, *15*, 1518.

(23) Perrin, D. D.; Armarego, W. L. F.; Perrin, D. R. *Purification of Laboratory Chemicals*, 2nd ed.; Pergamon: New York, 1980.

Cl₂): $\nu(\text{CO})$ (cm⁻¹) 1963 (w), 1932 (s), 1909 (w), 1740 (m). IR (hexanes): $\nu(\text{CO})$ (cm⁻¹) 1976 (s), 1947 (s), 1917 (s), 1753 (s).

Synthesis of $\{(\eta^5\text{-C}_5\text{H}_3)_2(\text{SiMe}_2)_2\text{Ru}_2(\text{CO})_3(\text{PPh}_3)\}$ (2c**).** A solution of **1** (30 mg, 0.053 mmol) in decane (1 mL) was reacted with PPh₃ (60 mg, 0.23 mmol) at 200 °C for 24 h, as in the preparation of **2a**. Two crystallizations of the resulting orange oil from CH₂Cl₂–hexanes gave **2c** (25 mg, 67%) as red crystals. ¹H NMR (400 MHz, CD₂Cl₂): δ 0.43 (s, 6 H, Si(CH₃)), 0.53 (s, 6 H, Si(CH₃)), 4.66 (d, $J = 2.4$ Hz, 2 H, Cp-*H*), 4.91 (m, 1 H, Cp-*H*), 5.44 (d, $J = 2.1$ Hz, 2 H, Cp-*H*), 5.72 (t, $J = 2.1$ Hz, 1 H, Cp-*H*), 7.53–7.78 (complex m, 15 H, P(C₆H₅)₃). ³¹P{¹H} NMR (161 MHz, CD₂Cl₂): δ 53 (s). IR (CH₂Cl₂): $\nu(\text{CO})$ (cm⁻¹) 1973 (vs), 1948 (m), 1917 (vs), 1735 (m). IR (hexanes): $\nu(\text{CO})$ (cm⁻¹) 1967 (vs), 1911 (vs).

Synthesis of $\{(\eta^5\text{-C}_5\text{H}_3)_2(\text{SiMe}_2)_2\text{Ru}_2(\text{CO})_4(\text{Cl})_2\}$ (3a**).** A solution of Cl₂, prepared by passing gaseous chlorine through CH₂Cl₂ (30 mL) for ~1 min, was added dropwise to a solution of complex **1** (120 mg, 0.22 mmol) in CH₂Cl₂ (60 mL). The reaction was monitored by IR spectroscopy and stopped when complex **1** was used up completely. The resulting solution was then concentrated at reduced pressure to ~5 mL, and hexanes (20 mL) was added to give complex **3a** (102 mg, 72%) as a yellow solid. ¹H NMR (400 MHz, CDCl₃): δ 0.24 (s, 6 H, Si(CH₃)), 0.59 (s, 6 H, Si(CH₃)), 5.34 (d, $J = 2.6$ Hz, 4 H, Cp *H*), 5.49 (t, $J = 2.6$ Hz, 2 H, Cp *H*). IR (hexanes): $\nu(\text{CO})$ (cm⁻¹) 2060 (vs), 2006 (vs). Anal. Calcd for C₁₈H₁₈Cl₂O₄Ru₂Si₂: C, 34.45; H, 2.89. Found: C, 34.87; H, 2.81.

Synthesis of $\{(\eta^5\text{-C}_5\text{H}_3)_2(\text{SiMe}_2)_2\text{Ru}_2(\text{CO})_4(\text{Br})_2\}$ (3b**).** When Br₂ (~5% solution in CH₂Cl₂) was reacted with complex **1** (120 mg, 0.22 mmol) in CH₂Cl₂ (60 mL), **3b** (141 mg, 85%; yellow solid) was obtained, using the same method as in the preparation of **3a**. ¹H NMR (400 MHz, CDCl₃): δ 0.21 (s, 6 H, Si(CH₃)), 0.60 (s, 6 H, Si(CH₃)), 5.21 (d, $J = 2.6$ Hz, 4 H, Cp *H*), 5.42 (t, $J = 2.6$ Hz, 2 H, Cp *H*). IR (hexanes): $\nu(\text{CO})$ (cm⁻¹) 2058 (vs), 2004 (vs).

Synthesis of $\{(\eta^5\text{-C}_5\text{H}_3)_2(\text{SiMe}_2)_2\text{Ru}_2(\text{CO})_4(\text{I})_2\}$ (3c**).** When I₂ (~5% solution in CH₂Cl₂) was reacted with complex **1** (120 mg, 0.22 mmol) in CH₂Cl₂ (60 mL), **3c** (132 mg, 71%; yellow solid) was obtained, using the same method as in the preparation of **3a**. ¹H NMR (400 MHz, CDCl₃): δ 0.27 (s, 6 H, Si(CH₃)), 0.56 (s, 6 H, Si(CH₃)), 5.32 (d, $J = 2.6$ Hz, 4 H, Cp *H*), 5.45 (t, $J = 2.6$ Hz, 2 H, Cp *H*). IR (hexanes): $\nu(\text{CO})$ (cm⁻¹) 2052 (vs), 2000 (vs).

Synthesis of $[(\eta^5\text{-C}_5\text{H}_3)_2(\text{SiMe}_2)_2\text{Ru}_2(\text{CO})_4(\mu\text{-Cl})]^+\text{TfO}^-$ (4a**).** A yellow solution of **1** (175 mg, 0.31 mmol) and AgOTf (89 mg, 0.35 mmol) in CH₂Cl₂ (30 mL) was titrated with a solution of chlorine in CH₂Cl₂, prepared as described in the synthesis of **3a**. The reaction was followed by IR until the starting complex **1** disappeared. The resulting red-brown suspension was filtered through a short pad of Celite, and the filtrate was layered with Et₂O (100 mL) to precipitate **4a** as bright orange cubic crystals (199 mg, 85%). ¹H NMR (400 MHz, CD₂Cl₂): δ 0.65 (s, 6 H, Si(CH₃)), 0.69 (s, 6 H, Si(CH₃)), 5.08 (t, $J = 2.0$ Hz, 2 H, Cp *H*), 5.93 (d, $J = 2.0$ Hz, 4 H, Cp *H*). ¹³C NMR (100 MHz, CD₂Cl₂): δ -3.57 (CH₃), 0.02 (CH₃), 79.89, 94.76, 106.27 (Cp), 194.17, 204.95 (CO). IR (CH₂Cl₂): $\nu(\text{CO})$ (cm⁻¹) 2077 (vs), 2069 (m), 2029 (s). Anal. Calcd for C₁₉H₁₈O₇-ClF₃Ru₂SSi₂: C, 30.79; H, 2.45. Found: C, 30.68; H, 2.43.

Synthesis of $[(\eta^5\text{-C}_5\text{H}_3)_2(\text{SiMe}_2)_2\text{Ru}_2(\text{CO})_4(\mu\text{-Br})]^+\text{TfO}^-$ (4b**).** When Br₂ (~5% solution in CH₂Cl₂) was reacted with complex **1** (175 mg, 0.31 mmol) and AgOTf (89 mg, 0.35 mmol) in CH₂Cl₂ (30 mL), **4b** (141 mg, 51%; orange solid) was obtained, using the same method as in the preparation of **4a**. ¹H NMR (400 MHz, CD₂Cl₂): δ 0.60 (s, 6 H, Si(CH₃)), 0.68 (s, 6 H, Si(CH₃)), 5.11 (t, $J = 2.0$ Hz, 2 H, Cp *H*), 5.91 (d, $J = 2.0$ Hz, 4 H, Cp *H*). IR (CH₂Cl₂): $\nu(\text{CO})$ (cm⁻¹) 2074 (vs), 2065 (m), 2026 (s).

Synthesis of $[(\eta^5\text{-C}_5\text{H}_3)_2(\text{SiMe}_2)_2\text{Ru}_2(\text{CO})_4(\mu\text{-I})]^+\text{TfO}^-$ (4c**).** When I₂ (~5% solution in CH₂Cl₂) was reacted with complex **1** (175 mg, 0.31 mmol) and AgOTf (89 mg, 0.35 mmol) in CH₂Cl₂ (30 mL), **4c** (191 mg, 78%; orange solid) was

obtained, using the same method as in the preparation of **4a**. ¹H NMR (400 MHz, CD₂Cl₂): δ 0.59 (s, 6 H, Si(CH₃)), 0.66 (s, 6 H, Si(CH₃)), 5.13 (t, $J = 2.0$ Hz, 2 H, Cp *H*), 5.89 (d, $J = 2.0$ Hz, 4 H, Cp *H*). IR (CH₂Cl₂): $\nu(\text{CO})$ (cm⁻¹) 2072 (vs), 2061 (m), 2025 (s).

Synthesis of *cis*- $\{(\eta^5\text{-C}_5\text{H}_3)_2(\text{SiMe}_2)_2\text{Ru}_2(\text{CO})_4(\mu\text{-SnCl}_2)\}$ (5**).** A solution of **1** (200.0 mg, 0.36 mmol) and SnCl₂ (300 mg, 1.0 mmol) in THF (100 mL) was heated to reflux for 30 h. The mixture was cooled to ambient temperature and chromatographed on an alumina column (20 × 1 cm), first using hexanes as the eluent and then a 1:5 (v/v) mixture of CH₂Cl₂ and hexanes, which eluted a yellow band containing **5** (193 mg, 74%). ¹H NMR (400 MHz, CDCl₃): δ 0.36 (s, 6 H, Si(CH₃)), 0.58 (s, 6 H, Si(CH₃)), 5.58 (d, $J = 2.6$ Hz, 4 H, Cp *H*), 5.64 (t, $J = 2.6$ Hz, 2 H, Cp *H*). ¹³C NMR (100 MHz, CDCl₃): δ -0.52 (CH₃), 0.73 (CH₃), 88.09, 94.97, 95.26 (Cp), 196.95 (CO). IR (hexanes): $\nu(\text{CO})$ (cm⁻¹) 2038 (s), 2023 (s), 1986 (vs), 1954 (w). Anal. Calcd for C₁₈H₁₈Cl₂O₄Ru₂Si₂Sn: C, 28.97; H, 2.43. Found: C, 28.95; H, 2.52.

Generation of $[(\eta^5\text{-C}_5\text{H}_3)_2(\text{SiMe}_2)_2\text{Ru}_2(\text{CO})_4]^{2-}$ (6**) and Synthesis of $\{(\eta^5\text{-C}_5\text{H}_3)_2(\text{SiMe}_2)_2\text{Ru}_2(\text{CO})_4[\mu\text{-Ti}(\eta^5\text{-C}_5\text{H}_3)_2]\}$ (**7**).** A solution of **1** (100.0 mg, 0.18 mmol) in THF (50 mL) was added to Na/Hg (50 mg/2 mL) and THF (20 mL). After the mixture was stirred for 20 h at ambient temperature, the resulting yellow-green solution contained mainly $[(\eta^5\text{-C}_5\text{H}_3)_2(\text{SiMe}_2)_2\text{Ru}_2(\text{CO})_4]^{2-}$ (**6**), as indicated by IR bands at 1928 (vs) and 1808 (vs) cm⁻¹. The solution was cannulated from the amalgam layer and added to a solution of $(\eta^5\text{-C}_5\text{H}_3)_2\text{TiCl}_2$ (37 mg, 0.15 mmol) in THF (30 mL). The resulting solution was stirred for 1 h; volatiles were removed under reduced pressure, and the residue was recrystallized from hexanes (20 mL) to give **7** as pale yellow crystals (83 mg, 53%). ¹H NMR (400 MHz, CDCl₃): δ 0.41 (s, 6 H, Si(CH₃)), 0.61 (s, 6 H, Si(CH₃)), 4.89 (br s, 10 H, Cp *H*), 5.21 (m, 4 H, Cp *H*), 5.42 (m, 2 H, Cp *H*). IR (hexanes): $\nu(\text{CO})$ (cm⁻¹) 1938 (vs), 1876 (vs). Anal. Calcd for C₂₈H₂₈O₄Ru₂Si₂Ti₂: C, 42.97; H, 3.61. Found: C, 42.03; H, 3.35. The extreme moisture sensitivity of **7** results in the unsatisfactory combustion analysis.

Reaction of $\{(\eta^5\text{-C}_5\text{H}_3)_2(\text{SiMe}_2)_2\text{Ru}_2(\text{CO})_4$ with Diphenylacetylene. Synthesis of $\{(\eta^5\text{-C}_5\text{H}_3)_2(\text{SiMe}_2)_2\text{Ru}_2(\text{CO})_2(\mu\text{-CO})\{\eta^1\eta^1\text{-}\mu_2\text{-C(Ph)C(Ph)}\}$ (8**), $\{(\eta^5\text{-C}_5\text{H}_3)_2(\text{SiMe}_2)_2\text{Ru}_2(\text{CO})\{\eta^2\eta^4\text{-}\mu_2\text{-C(Ph)C(Ph)C(Ph)C(Ph)}\}$ (**9**), and $\{(\eta^5\text{-C}_5\text{H}_3)_2(\text{SiMe}_2)_2\text{Ru}_2(\text{CO})\{\eta^2\eta^4\text{-}\mu_2\text{-C(=O)C(Ph)C(Ph)C(Ph)C(Ph)}\}$ (**10**).** The photolysis tube, equipped with a magnetic stir bar, was charged with **1** (200 mg, 0.36 mmol) and diphenylacetylene (140 mg, 0.79 mmol). Benzene (120 mL) was added, and the reaction tube was then fit with the cold finger (10 °C) and an oil bubbler. A slow flow of argon was maintained through the solution using a Teflon cannula while it was irradiated with stirring for 25 h. During this time the solution turned from yellow to red. Solvent was removed under vacuum; the resulting orange-brown residue was dissolved in hexanes (10 mL) and chromatographed on an alumina column (20 × 3 cm) with hexanes–CH₂Cl₂ (5:1) as the eluent. A yellow band was eluted and collected. Then, a pale orange band was eluted with hexanes–CH₂Cl₂ (1:1). Finally, a red-orange band was eluted with hexanes–CH₂Cl₂ (1:20). After vacuum removal of the solvents from the above three eluates, the residues were recrystallized from hexanes (eluates 1 and 3) or hexanes–CH₂Cl₂ (1:1) (eluate 2) at -20 °C. From the first fraction, 123 mg (58%, based on **1**) of orange crystalline **9** was obtained. ¹H NMR (400 MHz, C₆D₆): δ -0.62 (s, 6 H, Si(CH₃)), 0.36 (s, 6 H, Si(CH₃)), 4.89 (d, $J = 2.0$ Hz, 2 H, Cp *H*), 5.00 (d, $J = 2.0$ Hz, 2 H, Cp *H*), 5.52 (t, $J = 2.0$ Hz, 1 H, Cp *H*), 6.01 (t, $J = 2.0$ Hz, 1 H, Cp *H*), 6.52 (t, $J = 7.6$ Hz, 2 H, Ph), 6.72 (t, $J = 7.6$ Hz, 2 H, Ph), 6.82 (d, $J = 7.6$ Hz, 2 H, Ph), 6.87 (br s, 12 H, Ph), 7.09 (t, $J = 7.6$ Hz, 2 H, Ph), 7.31 (d, $J = 7.6$ Hz, 2 H, Ph), 7.46 (br s, 8 H, Ph). ¹³C NMR (100 MHz, C₆D₆): δ -4.60 (CH₃), 8.13 (CH₃), 82.49, 85.71, 90.39, 92.41, 93.71, 104.49 (Cp), 121.08, 126.01, 126.42, 126.51, 126.62 (br), 127.79, 131.65, 132.98 (br), 135.05, 139.88, 152.26, 158.90 (Ph, C-Ph), 208.54

(CO). IR (hexanes): $\nu(\text{CO})$ (cm^{-1}) 1969 (vs). Anal. Calcd for $\text{C}_{43}\text{H}_{38}\text{ORu}_2\text{Si}_2^{1/2}\text{C}_5\text{H}_{12}$: C, 63.17; H, 5.13. Found: C, 63.08; H, 5.16. From the second fraction, 27 mg (12%, based on **1**) of orange crystalline **8** was obtained. ^1H NMR (400 MHz, C_6D_6): δ 0.12 (s, 3 H, Si(CH_3)), 0.23 (s, 3 H, Si(CH_3)), 0.26 (s, 3 H, Si(CH_3)), 0.21 (s, 3 H, Si(CH_3)), 4.41 (m, 2 H, Cp *H*), 4.89 (m, 2 H, Cp *H*), 5.23 (m, 2 H, Cp *H*), 6.56 (m, 4 H, Ph), 6.79 (m, 2 H, Ph), 6.91 (m, 4 H, Ph). IR (hexanes): $\nu(\text{CO})$ (cm^{-1}) 1983 (vs), 1935 (m), 1753 (m). Anal. Calcd for $\text{C}_{31}\text{H}_{28}\text{O}_3\text{Ru}_2\text{Si}_2$: C, 52.67; H, 3.99. Found: C, 53.01; H, 3.83. From the third fraction, 41 mg (21%, based on **1**) of red crystalline **10** was obtained. ^1H NMR (400 MHz, CDCl_3): δ -1.00 (s, 3 H, Si(CH_3)), 0.31 (s, 3 H, Si(CH_3)), 0.36 (s, 3 H, Si(CH_3)), 0.57 (s, 3 H, Si(CH_3)), 4.80 (m, 1 H, Cp *H*), 5.18 (m, 1 H, Cp *H*), 5.43 (m, 1 H, Cp *H*), 5.89 (t, $J = 2.2$ Hz, 1 H, Cp *H*), 6.02 (m, 1 H, Cp *H*), 6.89 (t, $J = 2.2$ Hz, 1 H, Cp *H*), 6.40–7.15 (complex array of signals, 19 H, Ph), 7.86 (d, $J = 8.4$ Hz, 1 H, Ph). ^{13}C NMR (100 MHz, C_6D_6): δ -4.42, -1.22, 6.76, 8.27 (CH_3), 63.21, 81.53, 86.78, 89.02, 89.06, 93.87, 96.93, 98.71, 98.78, 104.99 (Cp; 10 peaks), 110.19, 116.27, 117.20, 125.90, 125.95, 126.00, 126.08, 126.49, 126.70, 126.84, 127.36, 127.72, 131.33, 131.54, 132.47, 134.25, 134.99, 135.20, 139.88, 140.74, 141.95, 155.11, 175.58 (Ph, C–Ph; 23 out of 24 peaks), 203.10, 211.40 (CO, C(=O)–Ph). IR (hexanes): $\nu(\text{CO})$ (cm^{-1}) 1973 (vs), 1601 (w). Anal. Calcd for $\text{C}_{44}\text{H}_{38}\text{O}_2\text{Ru}_2\text{Si}_2^{1/2}\text{CH}_2\text{Cl}_2$: C, 59.42; H, 4.37. Found: C, 59.19; H, 4.59.

Reaction of $\{(\eta^5\text{-C}_5\text{H}_5)_2(\text{SiMe}_2)_2\text{Ru}_2(\text{CO})_4$ with Phenylacetylene. Synthesis of $\{(\eta^5\text{-C}_5\text{H}_5)_2(\text{SiMe}_2)_2\text{Ru}_2(\text{CO})_3(\mu\text{-C}=\text{CHPh})$ (12**) and $\{(\eta^5\text{-C}_5\text{H}_5)_2(\text{SiMe}_2)_2\text{Ru}_2(\text{CO})\{\eta^2:\eta^4\text{-}\mu\text{-C}(\text{H})\text{C}(\text{Ph})\text{C}(\text{H})\text{C}(\text{Ph})\}$ (Mixture of Isomers) (**13**).** The photolysis tube, equipped with a magnetic stir bar, was charged with **1** (200 mg, 0.36 mmol) and phenylacetylene (160 mg, 1.23 mmol). Benzene (120 mL) was added, and the reaction tube was then fitted with the cold finger (10 °C) and an oil bubbler. A slow flow of argon was maintained through the solution using a Teflon cannula while it was irradiated with stirring for 30 h. During this time the solution turned from yellow to red. Solvent was removed under vacuum; the resulting orange-brown residue was redissolved in hexanes (10 mL) and chromatographed on an alumina column (20 × 3 cm) with hexanes– CH_2Cl_2 (5:1) as the eluent. A yellow band was eluted and collected. Then, a pale orange band was eluted with hexanes– CH_2Cl_2 (1:5). After vacuum removal of the solvents from the above two eluates, the residues were recrystallized from hexanes at -20 °C. From the first fraction, 17 mg (8%, based on **1**) of the orange oily solid **13** was obtained as a mixture of three isomers. The ^1H NMR (400 MHz, C_6D_6) spectrum displays a complicated pattern of signals due to the presence of three unique geometrical isomers (see Discussion). IR (hexanes): $\nu(\text{CO})$ (cm^{-1}) 1977 (w), 1968 (vs). From the second fraction, 107 mg (72%, based on **1**) of yellow crystalline **12** was obtained. ^1H NMR (400 MHz, CD_2Cl_2): δ 0.40 (s, 3 H, Si(CH_3)), 0.49 (s, 3 H, Si(CH_3)), 0.55 (s, 3 H, Si(CH_3)), 0.68 (s, 3 H, Si(CH_3)), 5.59 (m, 1 H, Cp *H*), 5.61 (m, 1 H, Cp *H*), 5.70 (m, 1 H, Cp *H*), 5.73 (m, 1 H, Cp *H*), 6.23 (m, 1 H, Cp *H*), 6.37 (m, 1 H, Cp *H*), 7.10 (m, 1 H, Ph), 7.30 (m, 2 H, Ph), 7.61 (s, 1 H, C=CPh*H*), 7.62 (m, 2 H, Ph). ^{13}C NMR (100 MHz, CD_2Cl_2): δ -3.27 (CH_3), -3.00 (CH_3), 2.64 (2 CH_3), 91.81, 92.07, 93.03, 94.21, 94.71, 95.50, 107.98, 108.03, 109.48, 110.125 (Cp), 125.44, 128.47, 138.68, 141.00 (Ph), 201.02, 202.11, 241.36 (CO), 247.42 (C=CPh*H*). IR (hexanes): $\nu(\text{CO})$ (cm^{-1}) 2008 (vs), 1982 (m), 1819 (m). Anal. Calcd for $\text{C}_{25}\text{H}_{24}\text{O}_3\text{Ru}_2\text{Si}_2$: C, 47.60; H, 3.84. Found: C, 47.47; H, 4.12.

Crystallographic Structural Determination of 1. A yellow crystal of **1** with approximate dimensions 0.38 × 0.34 × 0.32 mm was selected under oil under ambient conditions and attached to the tip of a glass capillary. The crystal was mounted in a stream of cold nitrogen at 183(2) K and centered in the X-ray beam by using a video camera. The crystal evaluation and data collection were performed on a Bruker CCD-1000 diffractometer with Mo $\text{K}\alpha$ ($\lambda = 0.71073$ Å) radiation and diffractometer to crystal distance of 5.08 cm. The initial cell constants were obtained from three series of ω scans at different starting angles. Each series consisted of 20 frames collected at intervals of 0.3° in a 6° range about ω with an exposure time of 10 s per frame. A total of 93 reflections was obtained. Reflections were successfully indexed by an automated indexing routine in the SMART program. The final cell constants were calculated from a set of 5689 strong reflections from the actual data collection. The data were collected by using the hemisphere data collection routine. Reciprocal space was surveyed to the extent of 1.8 hemispheres to a resolution of 0.80 Å. A total of 8075 data were harvested by collecting three sets of frames with 0.3° scans in ω with an exposure time of 20 s per frame. These highly redundant data sets were corrected for Lorentz and polarization effects. The absorption correction was based on fitting a function to the empirical transmission surface as sampled by multiple equivalent measurements.²⁴

Systematic absences in the diffraction data were consistent with space groups Cc and $C2/c$, but only the latter centrosymmetric space group $C2/c$ yielded chemically reasonable and computationally stable results in refinement.²⁵ A successful solution by direct methods provided most non-hydrogen atoms from the E map. The remaining non-hydrogen atoms were located in an alternating series of least-squares cycles and difference Fourier maps. All non-hydrogen atoms were refined with anisotropic displacement coefficients. All hydrogen atoms were included in the structure factor calculation at idealized positions and were allowed to ride on the neighboring atoms with relative isotropic displacement coefficients. Each molecule occupies a crystallographic 2-fold axis. The final least-squares refinement of 120 parameters against 2063 data resulted in residuals R (based on F^2 for $I \geq 2\sigma$) and R_w (based on F^2 for all data) of 0.0174 and 0.0457, respectively. The final difference Fourier map was featureless.

X-ray data for complexes **2a**, **3c**, **5**, **9**, **10**, and **12** were obtained in a similar manner, unless stated otherwise in the Supporting Information.

Acknowledgment. This work was supported by the National Science Foundation through Grant No. CHE-9816342.

Supporting Information Available: Tables giving crystallographic data for **1**, **2a**, **3c**, **5**, **9**, **10**, and **12**, including atomic coordinates, bond lengths and angles, and anisotropic displacement parameters. This material is available free of charge via the Internet at <http://pubs.acs.org>.

OM010674Y

(24) Blessing, R. H. *Acta Crystallogr.* **1995**, *A51*, 33–38.

(25) All software and sources of the scattering factors are contained in the SHELXTL (version 5.1) program library (G. Sheldrick, Bruker Analytical X-ray Systems, Madison, WI).